Division 2, National Defense Research Committee

of the

Office of Scientific Research and Development

CONCRETE PENETRATION

by

Richard A. Beth

NDRC Report No. A-319
OSRD Report No. 4856

Division 2, National Defense Research Committee
of the
Office of Scientific Research and Development

CONCRETE PENETRATION

by

Richard A. Beth

NDRC Report No. A-319
OSRD Report No. 4856

Submitted by

Walker Bleakney
Walker Bleakney, Supervisor
Princeton University Station

Ralph J. Slutz
R. J. Slutz, Technical Aide
Division 2
Effects of Impact and Explosion

Approved on March 20, 1945
for submission to the Committee

The NDRC Technical Reports Section
for armor and ordnance edited
this report and prepared it for duplication.

Requests for additional copies should be addressed through liaison channels to:
National Defense Research Committee
Technical Reports Section
Room 4724, Munitions Building
Washington 25, D.C.

Preface

The work described in this report is pertinent to the project designated by the War Department Liaison Officer as OD-75 and to the project designated by the Navy Department Liaison Officer as NO-11. The report constitutes a progress report under Contract OEMsr-260 with Princeton University.

Initial distribution of copies

Nos. 1 to 17 to Liaison Office, OSRD;

Nos. 18 to 25 to Office of the Executive Secretary, OSRD;

No. 26 to R. C. Tolman, Vice Chairman, NDRC;

No. 27 to J. P. Baxter, III, Historian, OSRD;

Nos. 28 and 29 to E. B. Wilson, Jr., Chief, Division 2;

No. 30 to W. Bleakney, Deputy Chief, Division 2;

No. 31 to M. P. White, Technical Aide, Division 2;

No. 32 to H. L. Bowman, Member, Division 2;

No. 33 to W. E. Lawson, Member, Division 2;

No. 34 to D. P. MacDougall, Member, Division 2;

No. 35 to S. A. Vincent, Member, Division 2;

No. 36 to J. von Neumann, Member, Division 2;

Nos. 37 and 38 to Division 2 Library, Princeton University;

No. 39 to Office of Field Service, OSRD (J. E. Burchard);

No. 40 to Ordnance Department Liaison Officer with NDRC;

Nos. 41 and 42 to Bureau of Ordnance (Research and Development Division, Re3);

No. 43 to Aberdeen Proving Ground (Ballistic Research Laboratory);

Nos. 44 to 48 to Liaison Office, OSRD, for transmittal to Division 2 London Representative; H. P. Robertson; Road Research Laboratory; Armament Research Department; Ministry of Home Security;

No. 49 to Army Ground Forces Liaison Officer with NDRC;

No. 50 to N. M. Newmark, Consultant, Division 2;

No. 51 to A. H. Taub, Consultant, Division 2;

No. 52 to L. H. Adams, Chief, Division 1;

No. 53 to H. B. Allen, Deputy Chief, Division 1;

Nos. 54 and 55 to Corps of Engineers (Lt. Col. W. J. New);

No. 56 to WDLO w/NDRC for transmittal to Col. P. Schwartz, Air Ordnance Officer, European Theater;

No. 57 to Aberdeen Proving Ground (Maj. J. S. Lieb);

No. 58 to Joint Target Group;

No. 59 to Office of Field Service, OSRD (V. V. Sides);

No. 60 to Experimental Officer, Naval Proving Ground;

No. 61 to Target Analysis Section, Joint Intelligence Center, Pacific Ocean Area (Lt. Comdr. T. C. Wilson);

No. 62 to Bureau of Aeronautics (Comdr. Eugene Tatom);

No. 63 to Frankford Arsenal (Lt. Col. C. H. Greenall);

No. 64 to R. A. Beth, Consultant, Division 2;

No. 65 to P. W. Bridgman, Harvard University;

Nos. 66 and 67 to Ordnance Department (Lt. Col. P. L. Christensen, S. Feltman);

Nos. 68 and 69 to Bureau of Ordnance (Comdr. T. J. Flynn, A. Wertheimer);

Nos. 70 and 71 to Bureau of Ships (Capt. H. G. Rickover, Comdr. C. H. Gerlach);

No. 72 to Army Air Forces (Lt. Col. J. M. Gruitch);

No. 73 to E. W. Engle, Carboloy Company;

No. 74 to Aberdeen Proving Ground (O. Veblen);

No. 75 to Watervliet Arsenal (Col. S. L. Conner);

Nos. 76 and 77 to Army Air Forces, Wright Field, Dayton, Ohio (Maj. J. P. AuWerter, Capt. R. T. Franzel);

No. 78 to David Taylor Model Basin (Capt. W. P. Roop);

No. 79 to Naval Proving Ground (Lt. Comdr. R. A. Sawyer);

No. 80 to Naval Research Laboratory (R. Gunn);

No. 81 to Bureau of Yards and Docks (Design Manager);

No. 82 to C. W. Curtis, Consultant, Division 2;

No. 83 to R. J. Emrich, Princeton University;

No. 84 to J. G. Stipe, Jr., Princeton University;

No. 85 to I. M. Freeman, Princeton University;

Nos. 86 to 95 to Operations Analysis Division, Management Control, HQ, AAF;

Nos. 96 and 97 to OSRD Liaison Office for transmittal to U.S. Strategic Bombing Survey (Lt. Col. J. W. Berretta);

No. 98 to Mina Rees, Technical Aide, Applied Mathematics Panel;

No. 99 to Watertown Arsenal (Col. H. H. Zornig).

CONTENTS

List of Figures

CONCRETE PENETRATION

Abstract

A large amount of concrete-penetration data has been collected in the past few years. It turns out that the available theories of penetration do not fit the data very well and, consequently: (a) makeshift empirical formulas have to be used in predicting concrete penetrations, and (b) no satisfactory basis exists for computing times, velocities, and forces during penetration since the "law of force" governing the variation of the force resisting the projectile during penetration is unknown.

The best way of improving our basic knowledge of penetration will be to obtain direct measurements of certain variables during penetration, provided that dependable experimental methods can be devised. A promising electromagnetic method is described in Appendix A. Since such direct measurements are not now available, the present report attempts to synthesize a more satisfactory theory by an indirect method.

The kind of penetration measurements that have been made (final penetration as a function of striking velocity), together with the laws of dynamics, are insufficient to determine uniquely the force law during penetration. The problem is, therefore, to supply additional assumptions concerning the force law that will be just sufficient to determine the force without leading to conflicts with the observations, as is the case with the assumptions made in the traditional theories of penetration.

This process is illustrated by assuming that the resisting pressure p depends only on the depth x and the velocity v at each instant, and that it is of the form $p = a(x) + bv^2$. The equation of motion is integrated and expressions are given for computing p, v, and the time t as functions of x during any particular penetration cycle. Furthermore, it is shown that if b is the same for two concretes and the ratio of their $a(x)$-functions is a constant C for all x, then the ratio of the striking energies required by the same projectile to reach any final depth x_1 in both concretes will also be equal to the constant C. This comparison principle agrees very well with caliber .50 penetration data for widely different concretes. This is in contrast to the lack of agreement that has been found for the commonly used assumption that there should be a constant ratio between penetrations in the two concretes independent of the striking velocity for which the comparison is made.

The new comparison principle is not restricted to the particular force law from which it is here derived (for example, see Appendix B); its validity rests mainly on its agreement with the observations. Using it, an average penetration curve is found from data for many different targets such that any particular penetration curve can be related to the average by means of a simple proportionality constant called the "concrete factor." Thus the accuracy of any particular penetration curve can be greatly enhanced and the

method of specifying the effect of concrete properties in penetration formulas is greatly improved.

Some new data (given in Appendix C) concerning the effect of projectile nose shape on penetration are analyzed according to the same comparison principle. It is found that the ratio of striking energies required by otherwise similar projectiles of different nose shapes to reach the same final depth x_1 in the same target is a constant, independent of x_1. The analysis of the data furthermore leads to a simple linear function of ogival nose height for representing the effect of nose shape in penetration formulas.

Further new data (Appendix C) concerning the effect of projectile mass on penetration are used to evaluate the constant b in the assumed force law. Appreciably better agreement with the data is secured for three widely different projectile masses on the same target than can be obtained either by applying the commonly used sectional-pressure assumption or by leaving out the bv^2 inertia term in the assumed force law.

Having thus obtained a satisfactory representation of the dependence of penetration on striking velocity, target concrete, projectile nose shape, and projectile mass on the basis of the assumed force law, the scope of the theory is illustrated by sample calculations of remaining kinetic energy, resisting pressure, and time during typical penetrations.

The theoretical consequences of a further generalization of the force law, namely $p = a(x)v^{2\lambda} + b(x)v^2$, are derived in Appendix B. The results do not upset the agreements with experiment found for the restricted theory; they may prove useful in fitting the data for different calibers (scale effect!), which is the principal remaining problem.

I. Introduction: The interrelation of theory and experiment

The purpose of this report is to review the present status of the problem of concrete penetration by projectiles and bombs, and to reexamine from the beginning the methods by which both theory and experiment may be brought to bear in obtaining answers to practical questions. "Theory" here means deductions from Newton's laws of motion, particularly the second law, $F = ma$, while "Experiment" consists mostly of observations of the final maximum penetration as a function of striking velocity for a large variety of target and projectile combinations. Other kinds of experimental observations -- especially those involving time, force, velocity, and displacement during penetration -- would indeed be useful, but these do not yet exist in sufficient quantity.

For convenience and clarity, penetration is distinguished from perforation: penetration refers to the entry of a missile into a massive target or into a target of sufficient thickness so that no visible effects appear on the back face; perforation generically refers to cases in which observable effects appear on the back face (thus cracking and scabbing of the back face are classed as perforation phenomena), while a complete perforation specifically refers to the passage of the missile through the target slab or plate.

In this report only penetration at normal incidence by a nondeforming projectile is under discussion unless otherwise stated. It is felt that the more complicated phenomena of perforation, of oblique penetration and perforation, and of deforming missiles can logically be best described and analyzed by comparison with normal, nondeforming penetration into the same target material. The discussion explicitly refers to concrete as the target material in this report, but it is thought that the methods of combining deductions from theory and inductions from experiment may, mutatis mutandis, be applicable to other target materials such as steel, armor, soil, and so forth, as well.

The diagram of Fig. 1 portrays in separate columns a number of the more obvious items of "Theory" and "Experiment" and their interrelations in the present status of the problem of penetration. The separation between the columns is almost complete in our present knowledge. The lines A, B, and C bridging the gap in the chart emphasize connections that should be examined in order to make progress toward a more unified structure.

The idealized separation into theory and experiment is, of course, not completely true in practice. For example, the empirical penetration formulas which have been constructed introduce the theoretical assumption that penetration is proportional to the projectile mass for a given target, striking velocity, caliber, and nose shape. Conversely, theoretically derived penetration formulas always contain certain parameters whose value is later to be fixed by reference to experimental penetration data.

The Robins-Euler and Poncelet theories[1/] are representative of the stage of our knowledge in the "Theory" column. Their inadequacy appears at

---

1/ See Part I of Ref. 1 for a summary of the classical theories of penetration. See List of References at the back of this report.

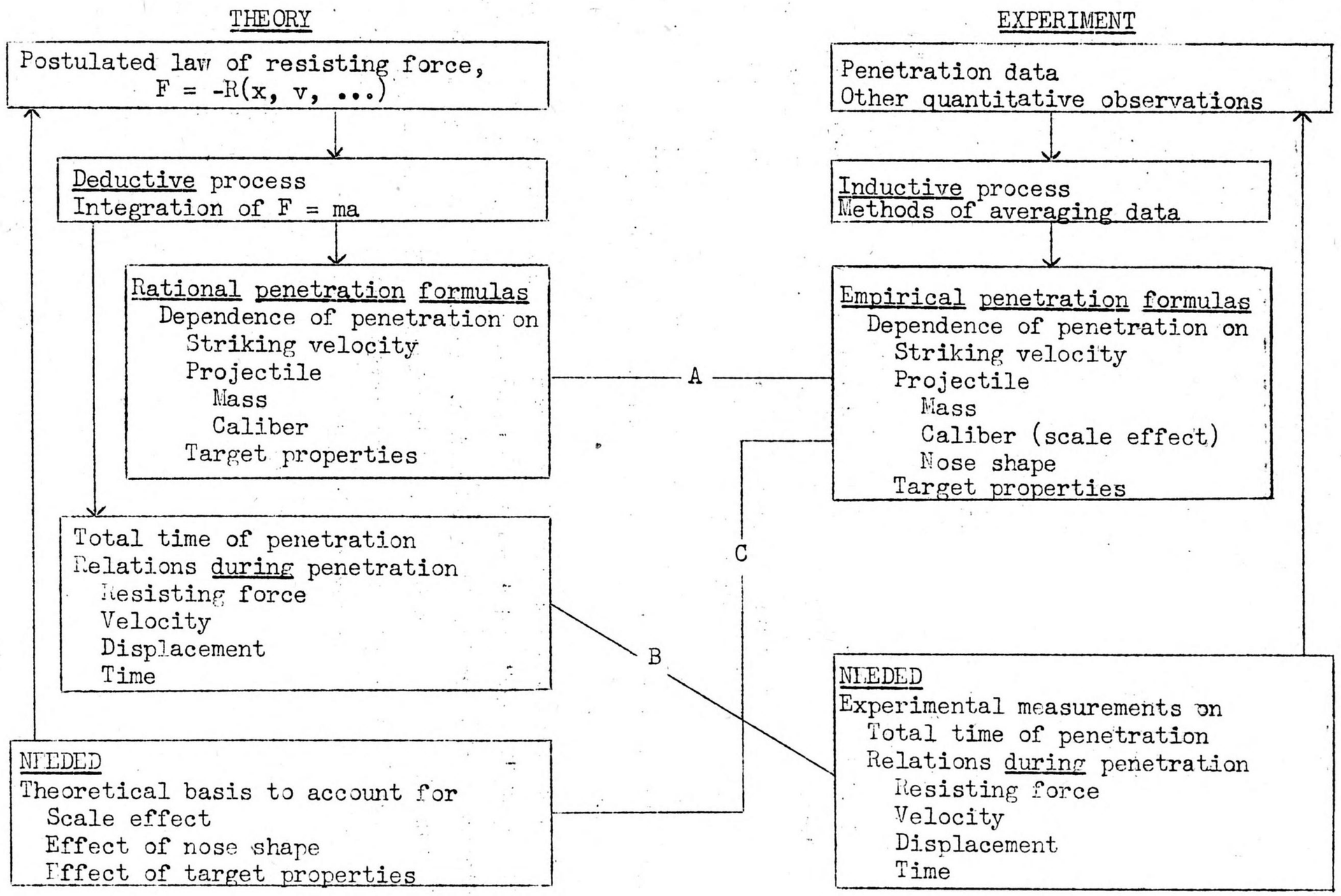

Fig. 1. Interrelation of theory and experiment in the penetration problem. The separation between the columns is almost complete in our present knowledge. Lines A, B, and C emphasize connections which should be examined in order to make progress toward a more unified structure.

For convenience and clarity, penetration is distinguished from perforation: penetration refers to the entry of a missile into a massive target or into a target of sufficient thickness so that no visible effects appear on the back face; perforation generically refers to cases in which observable effects appear on the back face (thus cracking and scabbing of the back face are classed as perforation phenomena), while a complete perforation specifically refers to the passage of the missile through the target slab or plate.

In this report only penetration at normal incidence by a nondeforming projectile is under discussion unless otherwise stated. It is felt that the more complicated phenomena of perforation, of oblique penetration and perforation, and of deforming missiles can logically be best described and analyzed by comparison with normal, nondeforming penetration into the same target material. The discussion explicitly refers to concrete as the target material in this report, but it is thought that the methods of combining deductions from theory and inductions from experiment may, mutatis mutandis, be applicable to other target materials such as steel, armor, soil, and so forth, as well.

The diagram of Fig. 1 portrays in separate columns a number of the more obvious items of "Theory" and "Experiment" and their interrelations in the present status of the problem of penetration. The separation between the columns is almost complete in our present knowledge. The lines A, B, and C bridging the gap in the chart emphasize connections that should be examined in order to make progress toward a more unified structure.

The idealized separation into theory and experiment is, of course, not completely true in practice. For example, the empirical penetration formulas which have been constructed introduce the theoretical assumption that penetration is proportional to the projectile mass for a given target, striking velocity, caliber, and nose shape. Conversely, theoretically derived penetration formulas always contain certain parameters whose value is later to be fixed by reference to experimental penetration data.

The Robins-Euler and Poncelet theories[1/] are representative of the stage of our knowledge in the "Theory" column. Their inadequacy appears at

---

1/ See Part I of Ref. 1 for a summary of the classical theories of penetration. See List of References at the back of this report.

once when an attempt is made to fit them to actual penetration observations over a sufficiently large range of striking velocities. The Pétry special case of the general Poncelet formula is very poor in this respect for concrete.

The empirical formulas[2] and nomograms[3] used at present in the United States and England for estimating concrete penetration illustrate the stage of our knowledge in the "Experiment" column. Neither their accuracy nor the scope of the knowledge so represented is satisfactory for all practical questions. They do not lead to a unique force law unless very strong additional assumptions are made, such as, for example, that the resisting force depends only on the instantaneous velocity v of the projectile (this has been followed up to some extent in England), or that it depends only on the instantaneous penetration x.[4] These current empirical formulas involve decimal or fractional powers of some of the variables and thus do not offer much promise for constructing a rational physical theory to account for them by integration of the equation of motion of the projectile. The most that can be said for them is that they provide systematic methods for averaging test data and for interpolation and extrapolation to values of the variables other than those actually observed. There are indications that these averaging methods need to be improved.

The net result of this situation is that we are not justified in being satisfied with our present understanding of concrete penetration. In

---

2/ See Refs. 2, 3, and 4.

3/ See Ref. 5.

4/ See Ref. 6, which forms a logical preface to the theory to be developed in the present report. Reference 6 deals with the computation of velocity v, time t, and resisting force R during penetration under the three simplest assumptions concerning the force law; namely, that the resisting force (a) is constant, which leads to the Robins-Euler theory, (b) depends only on v, which leads to the sectional-pressure theories of penetration, and (c) depends only on x, which leads to the sectional-energy theories of penetration. It is shown that either assumption (b) or (c) may be applied without internal contradiction to any given penetration curve, and that the use of the two assumptions results in the computation of different values of v and t during penetration. This illustrates the fact that a knowledge of the observed penetration curve alone does not imply a unique force law.

predicting penetrations, deviations of 15 to 30 percent may be encountered even within the ranges of the variables for which test data are available, and 50 percent or more for strong extrapolations such as large calibers and very low or very high caliber densities. The uncertainties in proceeding from normal penetrations to perforations and obliquities increase these possible errors. Of even greater practical consequence is the fact that we do not have a satisfactory basis for estimating forces and times -- forces which sometimes cause deformation or rupture of bombs and HE projectiles, forces required to initiate inertia-type fuzes, and times of penetration needed for optimum fuzing of explosive missiles.

Both the estimation of forces and times and the strengthening of the penetration formulas require a better knowledge of the variation of the force resisting the projectile during penetration than we now have. In the last analysis this improved knowledge will depend on direct experimental observations, as indicated in the lower right-hand corner of Fig. 1. Appendix A describes certain experimental methods with which promising preliminary trials have been made,[5/] but these experiments have now been discontinued because of the pressure of other work. It remains to see whether the indirect method of seeking a revised law of resisting force to eliminate obvious contradictions with the penetration data may not yield some improvement.

As has been noted, the theoretically derived penetration formulas in the literature[6/] do not have sufficient freedom in the form of undetermined parameters to permit adequate fitting of the available penetration data. On the other hand, empirical penetration formulas and curves do not, of themselves, lead to a unique law of resisting force. In other words, the path from left to right in Fig. 1 is overdetermined, while the path from right to left is underdetermined. This suggests:

A. Weakening the assumptions on the force function R so that the integrated equation of motion contains sufficient flexibility to permit its being fitted to the data. This may be done,

---

5/ See Ref. 7.

6/ See Ref. 1.

for example, by allowing the postulated resisting force R to contain appropriate undetermined functions as well as undetermined constants. The particular selection of R will then depend on physical plausibility, simplicity, and formal integrability of the equation of motion.

B. Strengthening the data analysis in order to evaluate the undetermined functions and parameters, and to provide, if possible, significant checks on the adequacy of the assumed form of the force function. An important aspect of this strengthening consists in finding improved methods of averaging and comparing penetration data for different targets and projectiles, thus reducing as far as possible the influence of random experimental errors in the quantitative results. The potential value of such improved methods may easily be equal to a large mass of new ad hoc data and should not be underestimated.

II. A theory of penetration

The remainder of this report is devoted to giving a specific illustration of the method of approach just described. We begin by postulating a generalized form of the Poncelet force law which is believed to be particularly appropriate for the accuracy and extent of the concrete penetration data available at present. The consequences of a further generalization of the Poncelet force law are developed in Appendix B.

We assume that the resisting force per unit maximum cross-sectional area of the projectile is of the form:

(1) $$\text{Resisting pressure} = p = R/A = a(x) + bv^2,$$

where

x = nose penetration of the projectile,
v = velocity of the projectile,
A = maximum cross-sectional area of the projectile.

This is significantly weaker and less restrictive than the usual Poncelet assumption in which the crushing parameter a is assumed constant;

nevertheless, it retains all the advantages of physical plausibility which have been adduced in favor of the Poncelet assumption and which have been adequately discussed elsewhere.[7]

The unspecified functional dependence of the crushing resistance a(x) on x can take account of the effect of (1) the pointed nose of the projectile entering the target, (2) crater formation and the lack of confinement of material near the target face, and (3) possible intrinsic variations of resistance with depth in the target due to curing,[8] pouring direction,[9] or other causes. On the other hand, the possibility that a is constant is not excluded.

The coefficient b in the term bv^2, which takes account of the inertial reaction of the displaced target material, may actually not be a constant as assumed here, but it is felt that the data of the kind required are at present not extensive or accurate enough to permit anything more than a mean value of b to be evaluated.

It is useful to make explicit the intended physical significance of b by introducing a dimensionless "inertia coefficient" γ as follows.[10] The increment of the projectile energy expended in overcoming the inertial reaction of the target material for a distance dx is

$$\Delta = Abv^2 dx.$$

The corresponding increment of volume swept out by the projectile is A dx. This volume represents a mass $(w'A\,dx)/g$ of target material, where w' is its weight per unit volume, and g is the acceleration due to gravity. If this mass had a velocity v, its kinetic energy would be

$$\Delta' = \frac{1}{2}\,\frac{w'A\,dx}{g}\,v^2.$$

7/ See pp. 12 to 15 in Ref. 1; pp. 42 and 43 in Ref. 8.

8/ See pp. 33 and 34 in Ref. 9.

9/ See p. 5 in Ref. 9.

10/ See p. 14, Ref. 1.

We define γ as the ratio of the true energy Δ expended by the projectile to this hypothetical kinetic energy Δ' gained by the target material:

$$\gamma = \frac{\Delta}{\Delta'} = \frac{2gb}{w'}, \tag{2}$$

or

$$b = \gamma \frac{w'}{2g}. \tag{3}$$

In order to summarize in a perspicuous form the quantitative physical relations implied by the assumed force law we eschew, for the moment, the formidable numerical factors which arise from the hybrid system of units later to be used for actual data computations. The following equations hold with any consistent set of units for the physical quantities involved (for example, the foot-pound-second system).

Using Eqs. (1) and (3), Newton's second law gives the equation of motion of the projectile in the target:

$$\frac{P}{g} v \frac{dv}{dx} = -p = -a(x) - \frac{\gamma w'}{2g} v^2, \tag{4}$$

where

$P = w/A$ = "sectional pressure" of the projectile,
w = weight of the projectile.

This is a first-order linear differential equation for the specific kinetic energy U of the projectile:

$$\frac{dU}{dx} + \gamma \frac{w'}{P} U = -a(x), \tag{5}$$

where $U [= Pv^2/2g]$ is the kinetic energy per unit cross-sectional area of the projectile. Using the initial conditions at the beginning of penetration, namely,

$x = 0$,
$v = v_o$ = striking velocity,
$U = U_o = Pv_o^2/2g$ = specific kinetic energy at striking,

to determine the constant of integration, the integral of Eq. (5) is

$$U = e^{-\gamma w' x/P} [U_o - u(x)], \tag{6}$$

where

$$u(x) \equiv \int_0^x a(x)\, e^{\gamma w' x/P}\, dx. \tag{7}$$

By inserting in Eq. (6) the final conditions,

$x = x_1$ = maximum nose penetration,

$v = 0$, and $U = 0$,

we obtain the relation between the specific striking kinetic energy and the maximum penetration:

$$U_o = u(x_1) = \int_0^{x_1} a(x)\, e^{\gamma w' x/P}\, dx. \tag{8}$$

This relation represents the experimentally observed "penetration curve." In terms of Eq. (6), which gives the remaining specific kinetic energy as a function of $\underline{x}$ during penetration, the resisting pressure $\underline{p}$ is

$$p = p(x) = -\frac{dU}{dx}; \tag{9}$$

the remaining velocity is

$$v = v(x) = \sqrt{\frac{2gU}{P}}; \tag{10}$$

and the time $\underline{t}$ after beginning of penetration is

$$t = t(x) = \int_0^x \frac{dx}{v} = \sqrt{\frac{P}{2g}} \int_0^x \frac{dx}{\sqrt{U}}. \tag{11}$$

Finally, from Eq. (7):

$$a(x) = e^{-\gamma w' x/P} \frac{du}{dx}. \tag{12}$$

In principle the evaluation of these quantities from existing penetration data is possible as follows. The observed penetration curve in the form of Eq. (8) gives directly the function u(x), defined in Eq. (7). The value of $\underline{\gamma}$ is derived from penetration curves u(x) for geometrically

similar projectiles (same caliber and shape) of different masses (different P) on the same target [same a(x) and w']. The remaining quantities -- p(x) v(x), t(x), and a(x) -- can then be found from u(x) and γ by using Eqs. (6) (9), (10), (11), and (12).

In the shot-by-shot computation and reduction of experimentally observed penetration data the following hybrid system of units is useful and convenient. It avoids the use of awkward numerical factors and powers of ten in stating velocities, energies, and so forth, and data for different calibers are at once brought to a common basis to facilitate intercomparison.

Symbol	Unit	Definition
w	lb	Weight of projectile.
d	in.	Maximum diameter of projectile (caliber).
v	ft/sec	Projectile velocity.
x	ft	Nose penetration.
X	in.	Nose penetration; thus X = 12x.
s	--	Specific gravity of target material.

We define the following derived quantities:

V	10^3 ft/sec	Projectile velocity; V = v/1000.
D	lb/in.^{3}	"Caliber density"; D = w/d^3
E	[10^3 ft/sec]^2 lb/in.^{3}	"Caliber energy"; E = DV^2
z	--	"Caliber penetration," that is, nose penetration in calibers; z = X/d = 12x/d.

In these terms the specific kinetic energy of the projectile is

$$U = \frac{2 \times 10^6}{\pi g} Ed = 19787 Ed \text{ ft-lb/in}^2, \tag{13}$$

and the experimentally observed "penetration curve" corresponding to Eq. (8) is

$$E_o = f(z_1). \tag{14}$$

The pure number w'x/P occurring in the exponents of the theoretical formulas is, physically, the dimensionless ratio of the mass of the target material displaced from the bullet hole to the mass of the bullet.

Subtracting a "nose correction" $\underline{\Delta\ell}$ (in.) from the nose penetrations seems appropriate in order to get a true estimate of the actual volume of the bullet hole.[11/] With

$$z_c = z - (\Delta\ell/d),$$

we get

$$\frac{w'}{P} x = 0.02837 \frac{s}{D} z_c = \text{a pure number.}$$

Hence, the mass dependence factor in the formulas is

$$(15) \qquad \mu(z) = e^{-\gamma w' x/P} = e^{-0.02837 \gamma s z_c/D} = 10^{-0.01232 \gamma s z_c/D},$$

where $\underline{\gamma}$ is the dimensionless "inertia coefficient" as previously defined.

Corresponding to Eq. (6) we have the caliber energy as a function of depth during penetration:

$$(16) \qquad E = \mu(z)[E_o - f(z)].$$

The instantaneous resisting pressure, Eq. (9), is

$$(17) \qquad p = - \frac{24 \times 10^6}{\pi g} \frac{dE}{dz} = - 237440 \frac{dE}{dz} \text{ lb/in}^2$$

and, similarly, the crushing resistance, Eq. (12), is

$$(18) \qquad a = 237440 \mu(z) \frac{df}{dz} \text{ lb/in}^2$$

From Eq. (16) we get for the velocity during penetration, Eq. (10),

$$(19) \qquad V = \sqrt{E/D} \ 10^3 \text{ ft/sec},$$

and for the time of penetration, Eq. (11),

$$(20) \qquad t = \frac{d\sqrt{D}}{12000} \int_o^z \frac{dz}{\sqrt{E}} \text{ sec.}$$

III. The penetration curves for different concretes

In the new notation the function f(z) has taken the place of u(x); the evaluation of all of the theoretical quantities depends on a knowledge

---

11/ See Appendix II, p. 87 in Ref. 8.

of f(z) and $\underline{\gamma}$ in addition to the directly determinable quantities $\underline{D}$, $\underline{d}$, $\underline{s}$, and $\underline{\Delta\ell}$. While f(z) is, in principle, obtained by plotting E_o against $z_1[= 12x_1/d]$ for any set of observed penetration data, the experimental errors are usually of the order of 5 to 10 percent, and the number of shots that can be taken on a given target is insufficient to define f(z) satisfactorily for numerical differentiation. Yet such differentiation is required in order to make a reasonable estimate of $\underline{\gamma}$ from data for otherwise similar bullets of different mass on the same target.

The following method of increasing the precision of f(z) by averaging and comparing the penetration curves for the same projectile on different targets seems to give excellent results. We introduce into the theory the following plausible supplementary assumption:

> For a group of similar concrete targets the individual crushing resistances a(z) bear constant ratios to one another for all values of $\underline{z}$.

We define the constant ratio of the crushing resistance a(z) for one of the concretes to the average crushing resistance $\bar{a}(z)$ for the whole group as the "Concrete Factor" $\underline{C}$ for that concrete:

$$C = \frac{a(z)}{\bar{a}(z)} = \text{constant, independent of } \underline{z}. \tag{21}$$

If the same projectile is used on similar concretes, s/D will be constant, and the mass dependence factor $\mu(z)$ in Eq. (15) will be the same for all targets of the group. We see from Eq. (7), or its analogue in our "practical" units,

$$f(z) = \frac{1}{237440}\int_o^z \frac{a(z)}{\mu(z)}\,dz, \tag{22}$$

that the relation between the penetration curve for one target of a group and the average penetration curve for all targets of the group is

$$f(z) = C\bar{f}(z), \tag{23}$$

where $\bar{f}(z)$ is the arithmetic average of the individual f(z) values for all members of the group at each value of $\underline{z}$. This, then, is the practical

expression of our supplementary assumption in the form in which it can be applied directly to experimental penetration data.

It is important to contrast Eq. (23) with the averaging methods heretofore employed for concrete data. Current empirical penetration formulas were constructed on the assumption, originally derived from the "sectional pressure" theories of penetration, that penetrations in different targets could be represented as being proportional to a universal function of striking velocity, the proportionality factor involving weight and caliber of the projectile as well as a penetration resistance parameter for the concrete. Penetration experiments at model scale[12] have shown that this assumption of a universal velocity dependence can give only a very rough representation of the data if the concrete quality is varied over a wide range. For example,[13] a weak concrete may show 3½ times the penetration obtained in a strong concrete at 1000 ft/sec and 5 times the penetration at 2000 ft/sec. The penetrations are obviously not proportional to the same velocity-dependence function for the two concretes. Correspondingly, the attempt to compare or average penetrations for fixed values of striking velocity[14] does not give very satisfactory results.

The considerations outlined above lead to an alternative suggestion, namely, that striking energies (or velocities, since D is assumed constant) be compared or averaged, for fixed values of penetration. As will be illustrated, this method of comparing and averaging penetration data seems to give much more satisfactory results than the old method with respect to both simplicity and accuracy.

The relation given by Eq. (23), together with the assumed constancy of γ, leads to a great simplification in computing the quantities in Eqs. (16) through (20), since they may be computed just once for the group average $\bar{f}(z)$, and then their values for any one of the concretes of the

---

12/ See Ref. 9.

13/ See p. 29 in Ref. 9.

14/ See pp. 22 to 28 in Ref. 9.

group (having the concrete factor $\underline{C}$) will be given by the relations

$$(24) \qquad C = \frac{E}{\bar{E}} = \frac{p}{\bar{p}} = \frac{a}{\bar{a}} = \left(\frac{V}{\bar{V}}\right)^2 = \left(\frac{t}{\bar{t}}\right)^2$$

for all values of $\underline{z}$ during penetration to the same maximum z_1.

The average penetration curve $\bar{f}(z)$ of Table I and Fig. 2 is based on a selection of twenty good sets of penetration data from the Concrete Properties Survey.[15/] A selection was originally made from the twenty-eight-day fog-cured concretes, but a comparison of the preliminary averages obtained indicated that data from the seven-day fog-cured target cubes could be included, which aided the extrapolation to values of $\underline{z}$ above 9.0 calibers. All of these data were obtained with caliber .50 E-6 hardened steel experimental projectiles with nearly the same caliber density; for this $\bar{f}(z)$-curve the average value of $\underline{D}$ was 0.5154 lb/in.^{3}, and the average value of s/D was 4.480 in.^{3}/lb. The values $\bar{f}(z)$ represent the arithmetic average of values for $z = 2,3,4,\ldots$ read from smooth curves drawn by eye on individual plots of the penetration data for each target. These averages were then normalized to $\bar{f}(z) \equiv 1.000$ at $z = 5.00$.

Table I. Normalized average penetration curve from selected Concrete Properties Survey data.

Average D = 0.5154 lb/in.^{3}; average s/D = 4.480 in.^{3}/lb

Caliber Penetration $\underline{z}$	Caliber Energy $\bar{f}$	Caliber Penetration $\underline{z}$	Caliber Energy $\bar{f}$	
2.00	0.245	9.00	2.149	
3.00	.467	10.00	2.445	partially extrapolated
4.00	.728	11.00	2.743	
5.00	1.000	12.00	3.043	
6.00	1.280	13.00	3.345	extrapolated
7.00	1.566	14.00	3.649	
8.00	1.856	15.00	3.955	

15/ See Table II-A in Ref. 9.

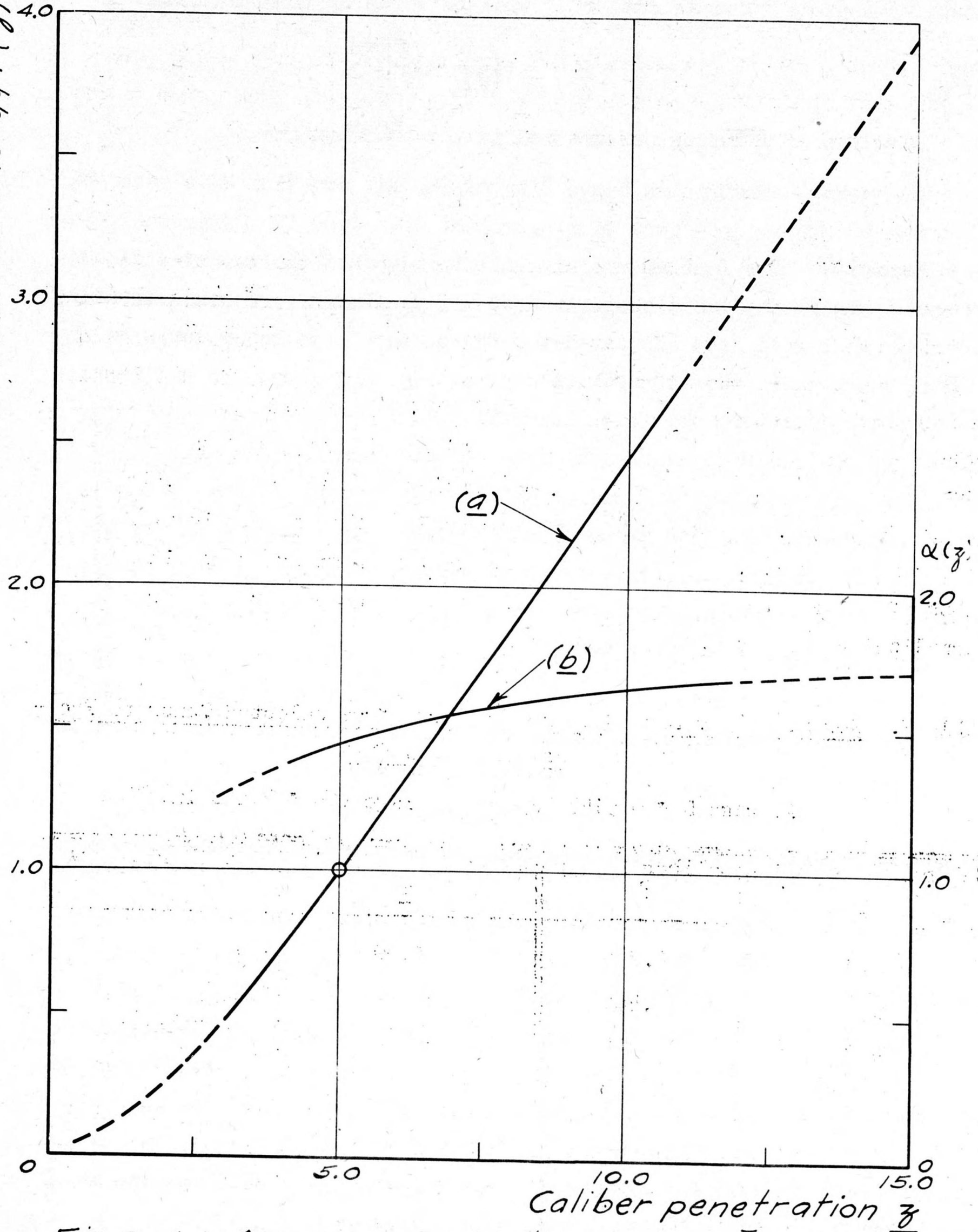

Fig. 2. (a) Average penetration curve $\bar{f}(z)$ based on a selection of 20 good sets of penetration data from the Concrete Properties Survey. (b) Approximate evaluation of $\alpha(z)$ obtained by numerical differentiation from Table I.

If a comparison is made between this f(z)-curve and a velocity dependence of penetration of the form $z = kV^{\alpha}$ by plotting f(z) on log-log paper, it is found that the slope $\underline{\alpha}$ varies with $\underline{z}$. An approximate evaluation of $\alpha(z)$ may be obtained by numerical differentiation from Table I,

$$\alpha(z) \sim 2 \frac{\bar{f}}{\bar{z}} \frac{\Delta z}{\Delta \bar{f}}, \tag{25}$$

The second curve on Fig. 2 was obtained in this way. It shows that the apparent value of $\underline{\alpha}$ will increase as deeper penetrations and less resistant concretes are considered. It has been pointed out[16] that this phenomenon may be the origin of the slightly different values of $\underline{\alpha}$ used in the British and American concrete-penetration formulas.

To test whether the proportionality relation, Eq. (23), between the data for a particular target and the average f(z)-curve holds, one may plot the observed caliber energy E_o for each shot against the caliber energy $\bar{f}(z_1)$ read from the smooth curve in Fig. 2 at the observed caliber penetration z_1. According to Eq. (23) the points should fall on or near a straight line through the origin; the slope of this line is the concrete factor $\underline{C}$. Assuming that the straight line passes through the origin and through the center of gravity of the points, its slope is

$$C = \frac{\Sigma E_o}{\Sigma \bar{f}(z_1)}, \tag{26}$$

the sums being taken over all of the shots considered. Using this value of $\underline{C}$ and Table I, the adjusted penetration curve may be obtained from Eq. (23).

If Eq. (26) is computed for the nine sets of data plotted in Figs. 2, 3, and 4 of Ref. 9, values of $\underline{C}$ ranging from 0.56 to 2.02 are obtained. The resulting adjusted penetration curves fit the data as well as, or better than, the curves resulting from the adjustment by the method given in the report cited; furthermore, the one-parameter relation, Eq. (23), is much simpler than the equation given on page 25 of that report for averaging and comparing penetration curves. Since the present method also has a better theoretical foundation it is to be preferred on all counts.

16/ See p. 27 in Ref. 9.

IV, The effect of nose shape on penetration

Some new caliber .50 data showing the effect of projectile nose shape and mass on penetration are given in Appendix C. These data were obtained during the work of the Concrete Properties Survey at Princeton, the same equipment and methods being used as described in the report on that test.[17/]

Along with the data for each special projectile, comparison data for standard caliber .50 E-6 projectiles were obtained on the same concrete, the sets of five target cubes being identically made on the same day, cured together, and tested for penetration at the same age of 28 days.

If, in line with the previous work, we compare caliber energies for the same depth of penetration we find that, within the accuracy of these data, the following empirical rule holds:

> For two projectiles of the same mass and caliber, but of different nose shape, penetrating the same concrete target, the ratio of striking caliber energies required to achieve a given depth of nose penetration is a constant, independent of the penetration depth for which the comparison is made.

We may, therefore, define a "Nose Shape Factor" $\underline{N}$ by which the actual caliber energy $E_o[= f(z_1)]$ should be multiplied to find the caliber energy required by a standard projectile with the same mass and caliber to reach the same final depth of nose penetration z_1. Combining this with Eq. (23), we have:

$$Nf(z) = C\bar{f}(z), \tag{27}$$

where $N \equiv 1.000$ for the standard projectile. Thus Eq. (23) is a special case of the more general Eq. (27). The standard caliber .50 E-6 projectile used in these tests has a 1.50 caliber radius ogival nose.

Table II gives a summary of the results concerning the effect of nose shape on penetration derived from the data of Appendix C. For projectiles with ogival noses the numerical value $\underline{n}$ of the radius of ogive in calibers

---

17/ See Ref. 9, especially Appendices A and B.

Table II. Summary of the effect of nose shape on penetration.

Target Cube No.	Ogival Nose Radius n (calibers)	Nose Height h (calibers)	C/N	Nose Factor N	Mean Caliber Density, D (lb/in.^{3})	s/D
B3B 3-7	1.50	1.118	1.115[a]	1.000	0.5215	4.43
B3B 3-7	Flat	0	1.580	0.706	.5046	4.58
B3B 13-17	1.50	1.118	0.986[a]	1.000	.5169	4.48
B3B 13-17	0.50	0.500	1.173	0.841	.4995	4.64
B3B 13-17	Flat	0	1.435	0.687	.5037	4.60
B3B 20-24	1.50	1.118	1.211[a]	1.000	.5134	4.52
B3B 20-24	3.10	1.688	1.050	1.153	.5434	4.27

a/ This is the concrete factor C for the standard projectile for which N = 1.00.

is listed in the second column; the word "Flat" is entered for square-ended slugs. For the ogival projectiles the nose height h in calibers is computed from[18]

(28) $$h = \sqrt{n - 0.25} \text{ calibers.}$$

The value of C/N given in the fourth column was computed by the method of Eq. (26), a few obviously poor points being discarded. For each set of target cubes the concrete factor C is the underlined value of C/N as listed for the standard projectile for which N = 1.000. The value of N for each of the other projectiles on the same concrete is obtained from C/N by using this value of C. The last two columns give the mean caliber density D of the projectiles actually used and the quotient s/D occurring in the exponent of the mass-dependence factor, Eq. (15). No allowance was made for the variation of this factor in the calculations for the values of C and N in Table II.

The values of the nose factor N are plotted against the corresponding nose heights h in Fig. 3. The straight line drawn on the figure is

(29) $$N = 0.70 + 0.268h.$$

18/ See Appendix II, p. 87 in Ref. 8.

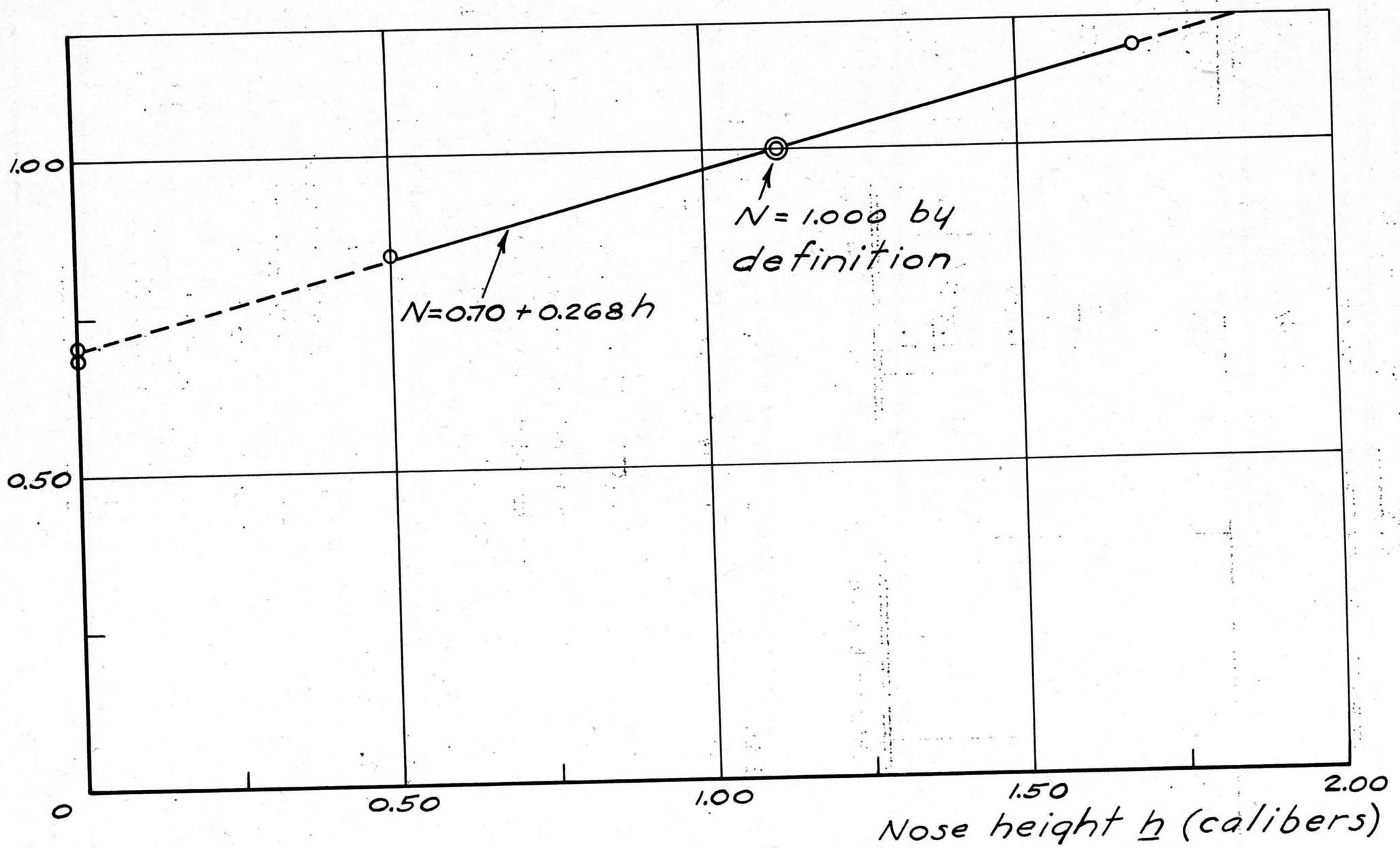

Fig. 3. Plot of nose factor N versus nose height.

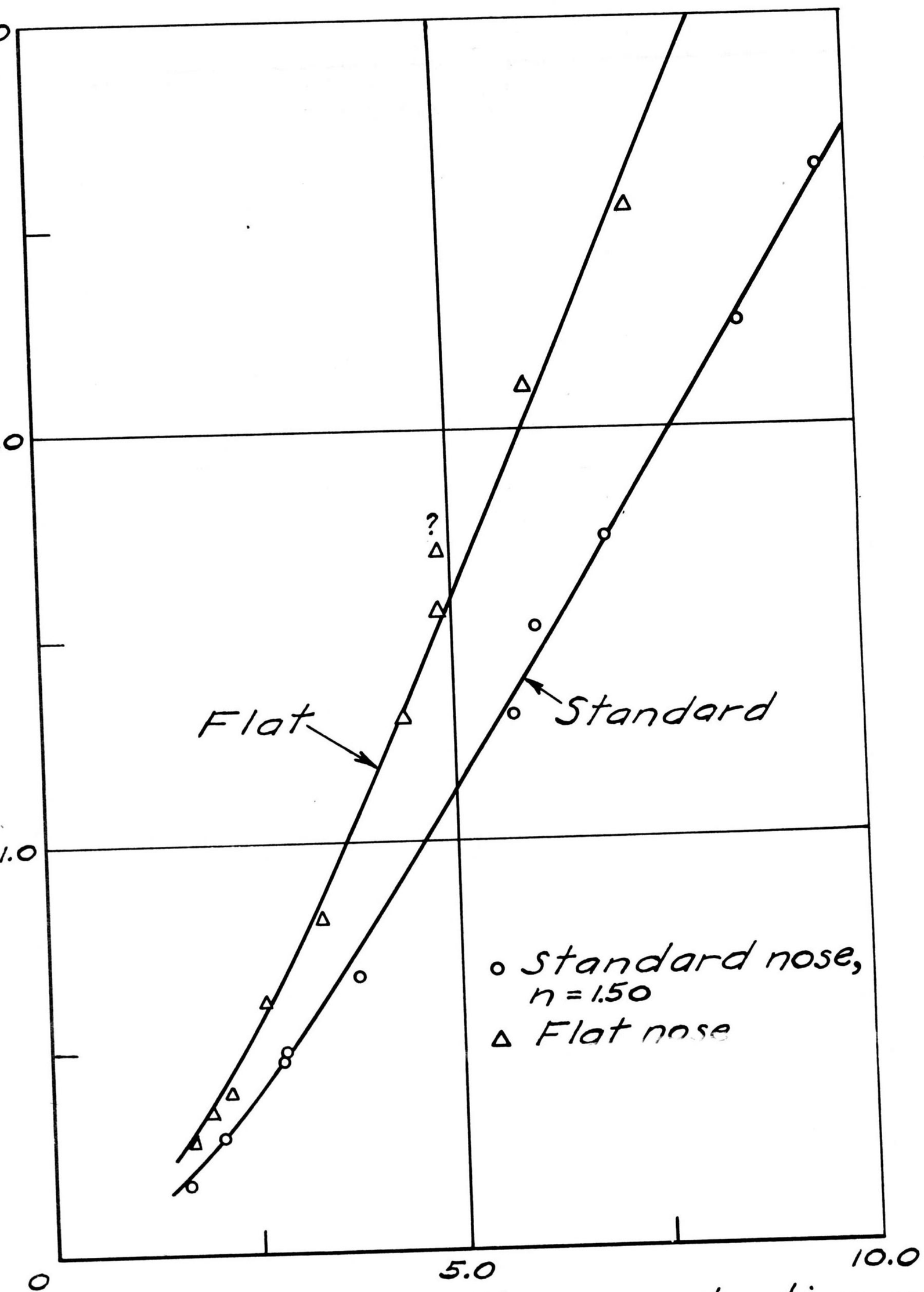

Fig. 4. Penetration data on target cubes B3B3-7.

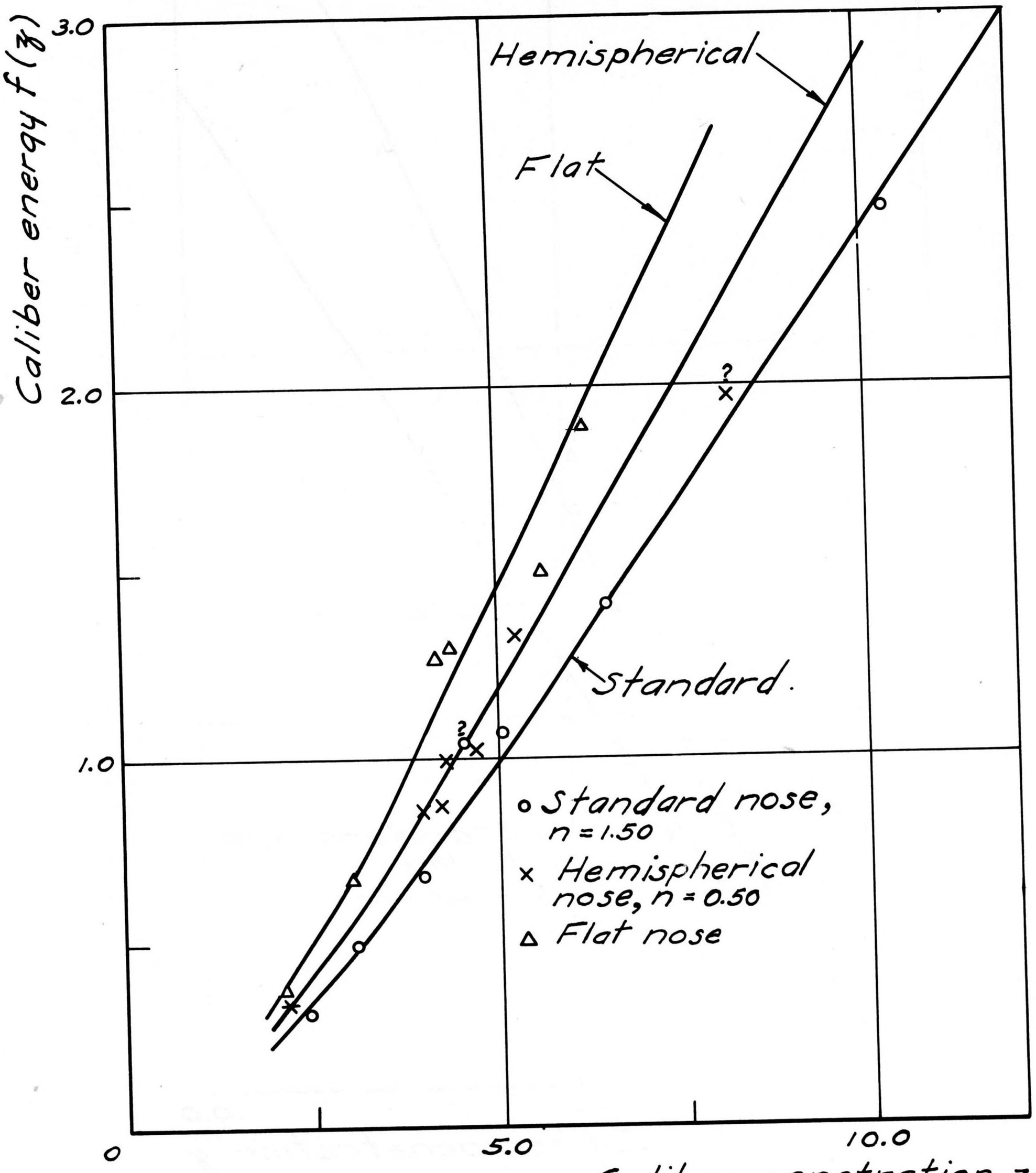

Fig. 5. Penetration data on target cubes B3B13-17.

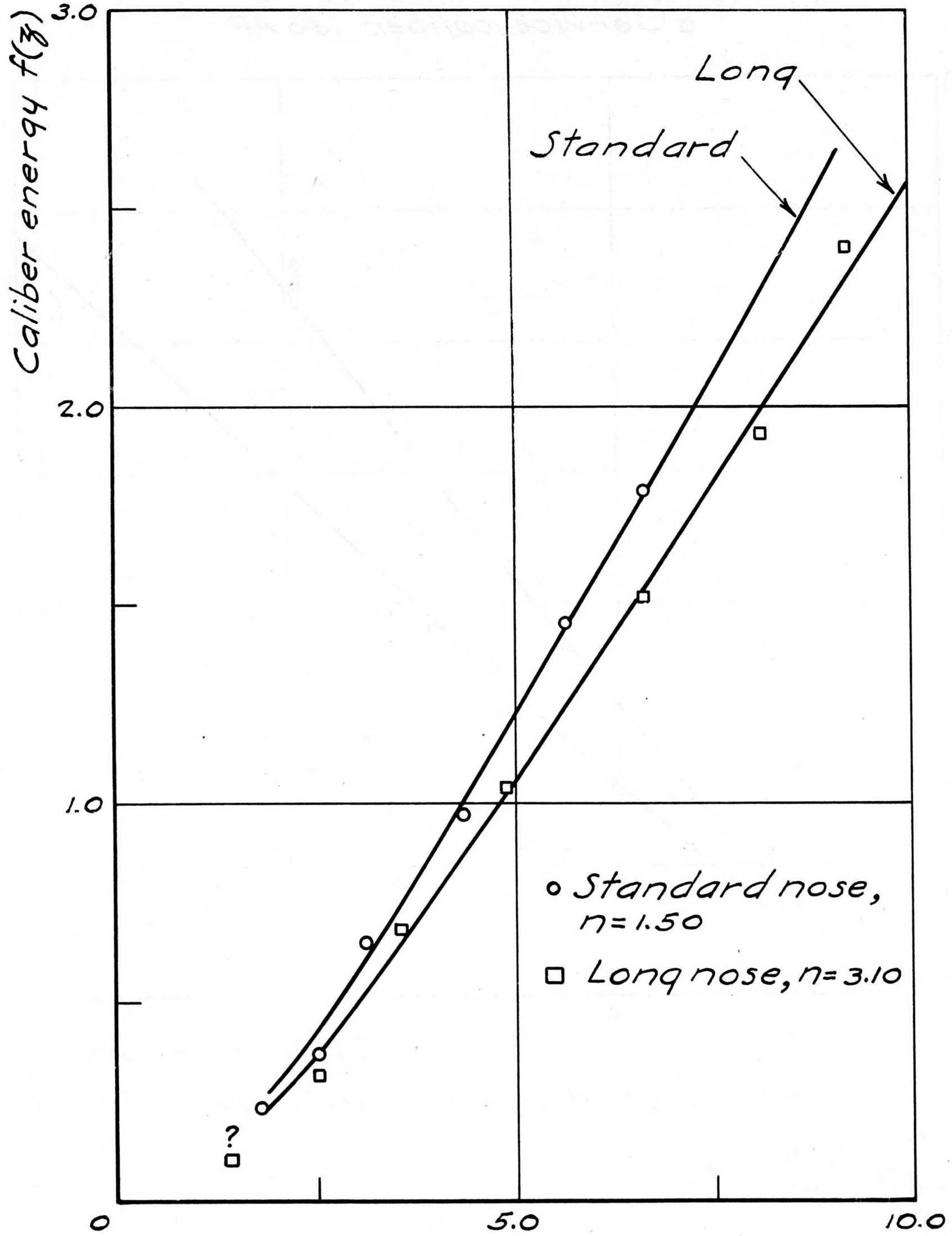

Fig. 6. Penetration data on target cubes B3B 20-24.

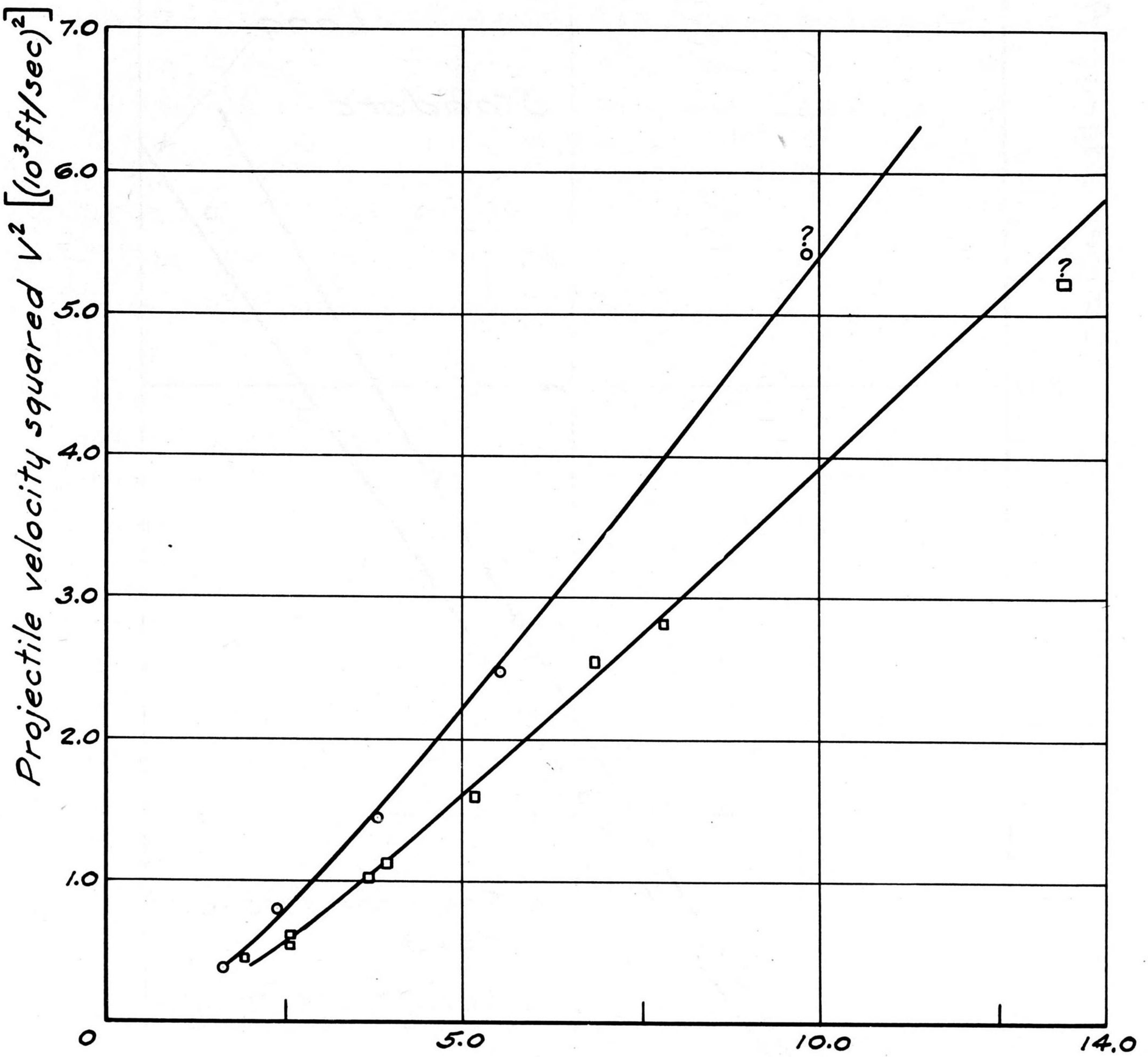

Fig. 7. Penetration data on target cubes B3B 25-29.

It is felt that this relation should give reasonably good estimates of the effect of nose shape on penetration for ogival projectiles even at larger calibers. The straight line, Eo, (29), in Fig. 3 is dashed from h = 0 to h = 0.50 because, strictly speaking, a tangent ogive is impossible with h < 0.5. The dashed continuation of the line above h = 1.70 represents an extrapolation.

Figures 4, 5, and 6 show plots of the data on which Table II is based, together with the smoothed penetration curves resulting from the adjustment. A question mark above the plotted point marks each of the four data points omitted in the adjustment.

We digress from the main argument for a moment to obtain an expression for the penetration of caliber .50 AP bullets in concrete. Figure 7 shows a plot of the data for the B3B 25-29 target cubes (Appendix C) comparing the penetrations of the service AP bullets with penetrations of our standard caliber .50 E-6 experimental projectiles on the same concrete.

The average mass of the AP bullets used was 45.58 gm, giving a nominal caliber density of 0.81 lb/in^3. However, the jacket of the service bullet is torn off within the first inch or two of penetration into concrete and then the observed maximum penetration is that of the core. Under these circumstances the initial projectile mass cannot be expected to have the same effect on penetration as in the case of a nondeforming projectile. Therefore V^2 rather than caliber energy is plotted as ordinate for this ad hoc comparison.

For this concrete the concrete factor, C = 1.139, was computed from Eq. (26) as before, using the data for the caliber .50 E-6 bullet. The curve drawn on the graph is

$$V^2 = C\bar{f}(z)/D = 1.937C\bar{f}(z),$$

since the average D = 0.5164 lb/in^3.

Using a method of calculation analogous to that of Eq. (26), but using the observed V^2-values rather than E_o in the numerator and thus ignoring the larger initial bullet mass, the constant for the curve

(30) $$V^2 = 1.403C\bar{f}(z)$$

as drawn for the caliber .50 AP projectiles was obtained. This equation will probably give good estimates of the penetration to be expected for the service bullet even for other values of the concrete factor C.

V. The dependence of penetration on projectile mass: Estimate of γ

According to the theory as outlined in Sec. II of this report, the projectile mass, expressed in terms of the caliber density D, affects the relation between striking velocity and penetration in two ways: (1) D enters in the calculation of the caliber energy E [= DV^2] and by writing the "penetration curve" in the form $E_o = f(z_1)$ this effect of projectile mass is taken into account in the simplest way. It may be expected that this takes care of the principal part of the influence of mass on penetration, as has been assumed in the work of Secs. III and IV. (2) D also enters in the integrand of Eq. (22) through the mass-dependence factor $\mu(z)$ defined in Eq. (15). Its effect here depends on the magnitude of the inertia coefficient γ, which remains to be evaluated.

Penetration data for caliber .50 E-6 bullets of three appreciably different masses on the same concrete (target cubes B3B 8-12) are given in Appendix C. The light-weight projectile was made by boring out the interior of a standard caliber .50 E-6 steel projectile before hardening; the heavy bullet was made of tungsten carbide to the same dimensions as the standard E-6 projectile. The 1.50-caliber-radius ogive gives $\Delta\ell/d = 0.49$ for the nose correction of these projectiles. The average specific gravity of the concrete of these targets was s = 2.312. The mass, caliber density, and s/D values were

Projectile Type	Average Mass (gm)	Average Caliber Density (lb/in^3)	s/D
Hollow	20.28	0.3609	6.41
Standard	29.07	0.5173	4.47
Tungsten carbide	58.70	1.0445	2.21

△ Hollow, D= 0.361 lb/in.^{3}
○ Standard, D= 0.517 lb/in.^{3}
□ Tungsten carbide, D= 1.045 lb/in.^{3}

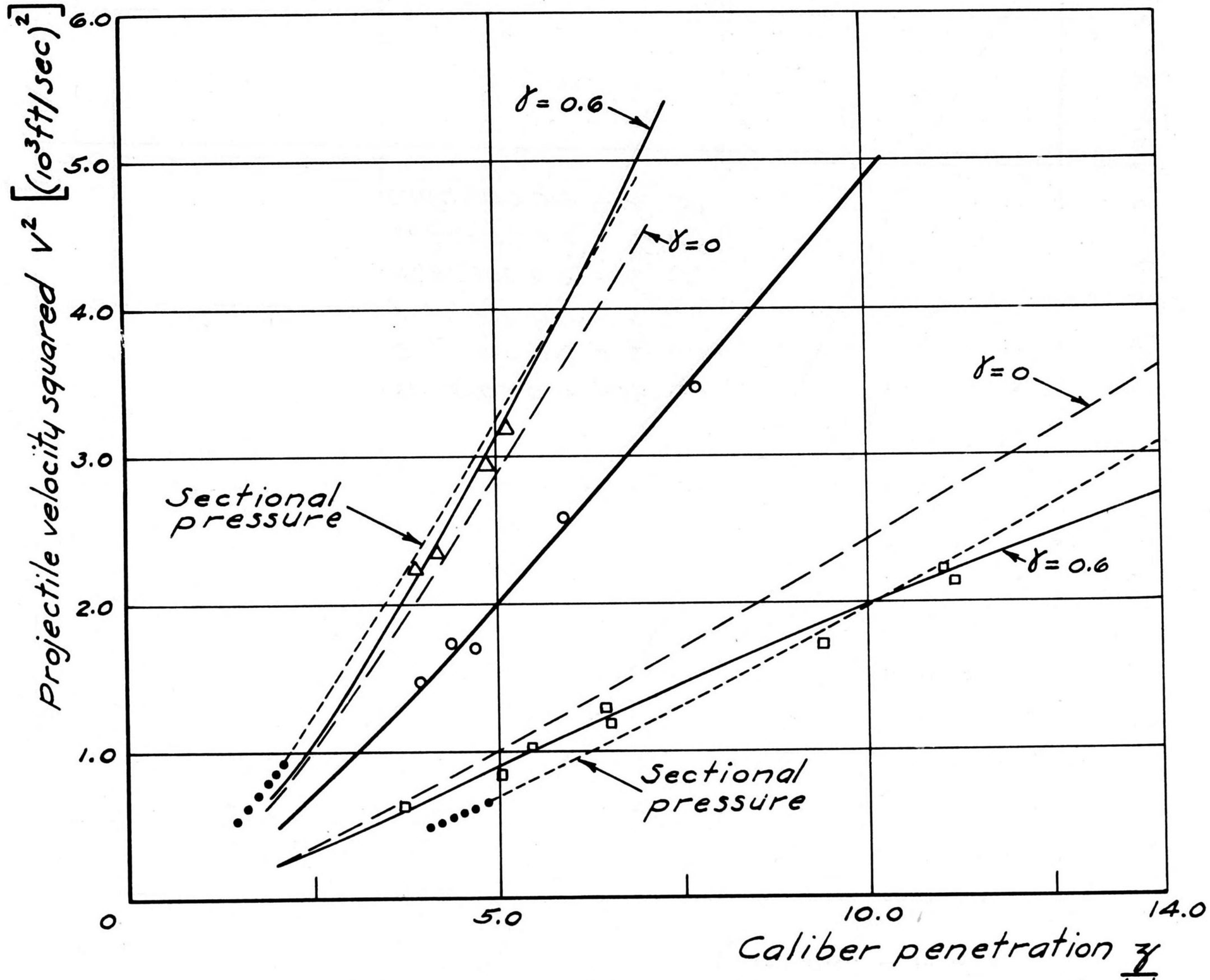

Fig. 8. Penetration data on target cubes B3B 8-12. Caliber .50 E-6 projectiles.

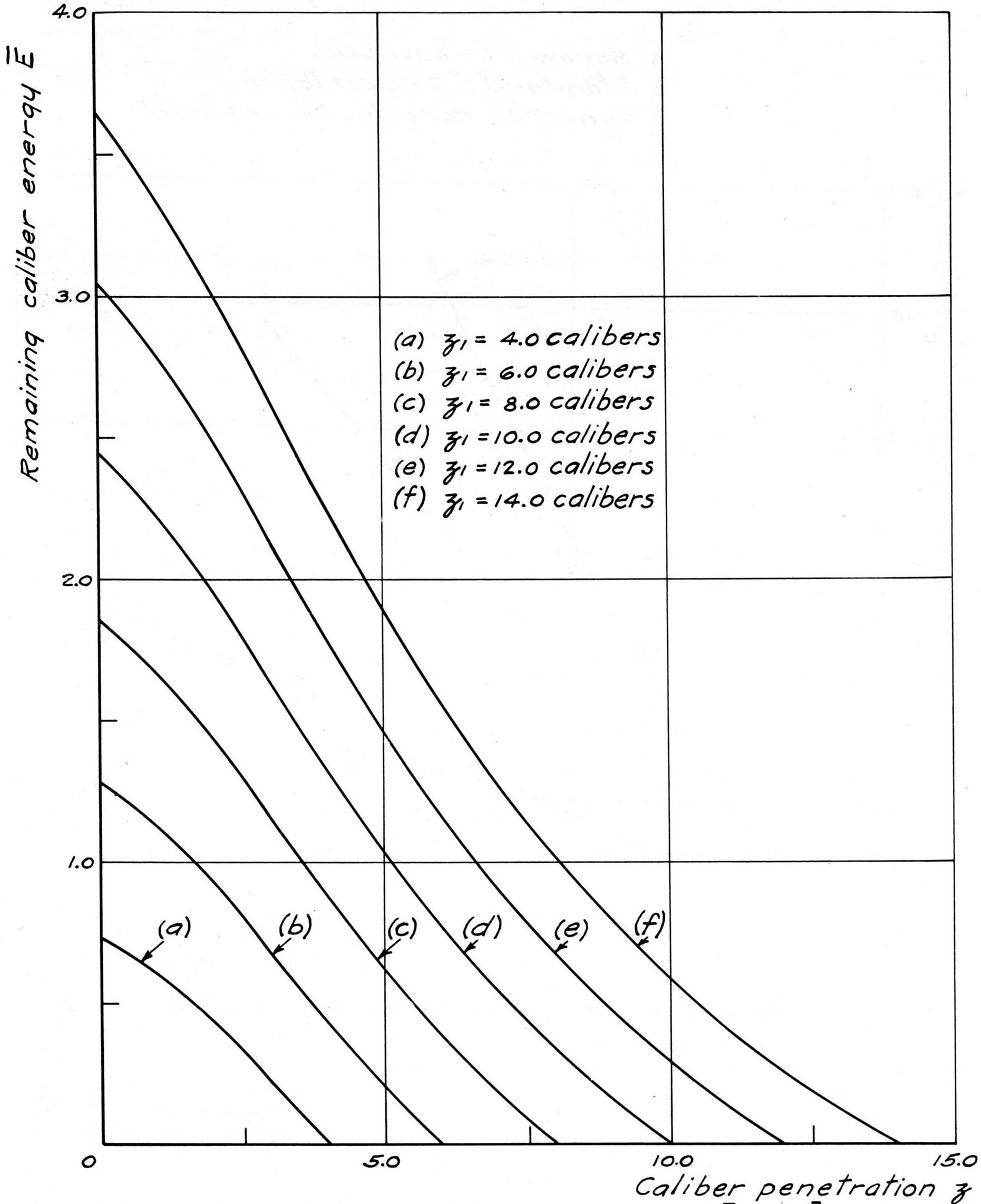

Fig. 9. Remaining caliber energy $E[=DV^2]$ versus instantaneous caliber penetration z during penetration. $\bar{E} = \mu(z)[\bar{f}(z_1) - \bar{f}(z)]$. The curves are based on the average caliber .50 E-6 penetration curve $f(z) = \bar{f}(z)$ given in Table I and Fig. 2, and on $\gamma = 0.6$.

In trying to get an estimate for $\underline{\gamma}$ from the penetration data for these three projectiles we can now take advantage of the greatly improved knowledge of the penetration curve for the standard projectile obtainable by means of the averaging methods of Sec. III.

Calculating the concrete factor from Eq. (26), we find, by Eq. (23),

$$f_1(z) = 1.027\bar{f}(z) \tag{31}$$

as the adjusted penetration curve for the standard projectile (denoted by the subscript 1), ignoring, as before, small differences in $\underline{D}$ and s/D. Using the subscript 2 to denote the quantities for a projectile of appreciably different mass and assuming that the crushing resistance a(z) remains the same, we have, from Eqs. (15), (18), and (22):

$$f_2(z) = \int_0^z \frac{df_1}{dz} \frac{\mu_1(z)}{\mu_2(z)}\, dz. \tag{32}$$

This integral can be evaluated for various assumed values of $\underline{\gamma}$ for both the hollow and the tungsten carbide projectiles. In the absence of an analytical expression for the penetration curve $f_1(z)$ the calculations require numerical differentiation and integration. Not only is this process greatly aided by relating $f_1(z)$ to the averaged curve $\bar{f}(z)$, but the approximations involved in taking finite intervals tend to compensate since the same intervals can be used for both the differentiation and the integration.

By a trial and error method based on Eq. (32) the estimate

$$\gamma = 0.6 \tag{33}$$

was obtained for the inertia coefficient for concrete from these data. The resulting fit is shown in Fig. 8 where $V^2 = f/D$ has been chosen as the ordinate in order to separate the curves and points more clearly. The dashed curves represent the values that would be obtained on the assumption $\gamma = 0$ and, by comparison with the others, illustrate the relative insensitivity of the computed values to the choice of $\underline{\gamma}$. It nevertheless seems significant that the <u>same</u> value, $\gamma = 0.6$, gives a good fit for both the hollow and the tungsten carbide projectiles. The dotted curves were obtained from $f_1(z)$

by using the old sectional-pressure hypothesis (without nose correction) that penetration is proportional to projectile mass. Even with this amount of data it will be seen that the new method gives distinctly better results.

VI. Kinetic energy, force, and time during penetration

It is now possible to compute values of E, p, a, v, and t during penetration from Eqs.(16) through (20) for any maximum penetration z_1 by using the penetration curve f(z) and the value of γ estimated in the previous section. In fact, we need only carry through the numerical calculations for the average penetration curve $\bar{f}(z)$: the results for any particular concrete can then be obtained by means of the simple ratios of Eq. (24); even for projectiles of somewhat different nose shape from the standard we may expect Eq. (24) to hold to a good approximation with C/N in place of C.

The curves given in Figs. 9, 10, and 11 are based on $\gamma = 0.6$ and the average caliber .50 E-6 penetration curve given in Table I and Fig. 2, for which s/D is about 4.5. If the ratio s/D of concrete specific gravity to projectile caliber density is appreciably different from this value the curves should be recalculated using an appropriately revised $\bar{f}(z)$-curve which could be obtained either experimentally or estimated by the method of Sec. V.

Figure 9 shows the caliber energy remaining at any depth during penetration computed from Eq. (16) for each of six maximum caliber penetrations, $z_1 = 4.0$, 6.0, 8.0, 10.0, 12.0, and 14.0 calibers.

Figure 10 shows the resisting pressure p computed from Eq. (17) as a function of depth during penetration for the same six maximum penetrations, and the crushing resistance of the concrete from Eq. (18) as a function of depth. The differentiations were performed numerically by plotting the average value for the z-intervals in Table I at the midpoint of each interval.

The time of penetration computed from Eq. (20) is presented in Fig. 11 in terms of the dimensionless parameter $v_o t/x$ plotted as a function of the instantaneous caliber penetration z. The calculations were made for the same six maximum penetrations as before. The dimensionless quantity $v_o t/x$

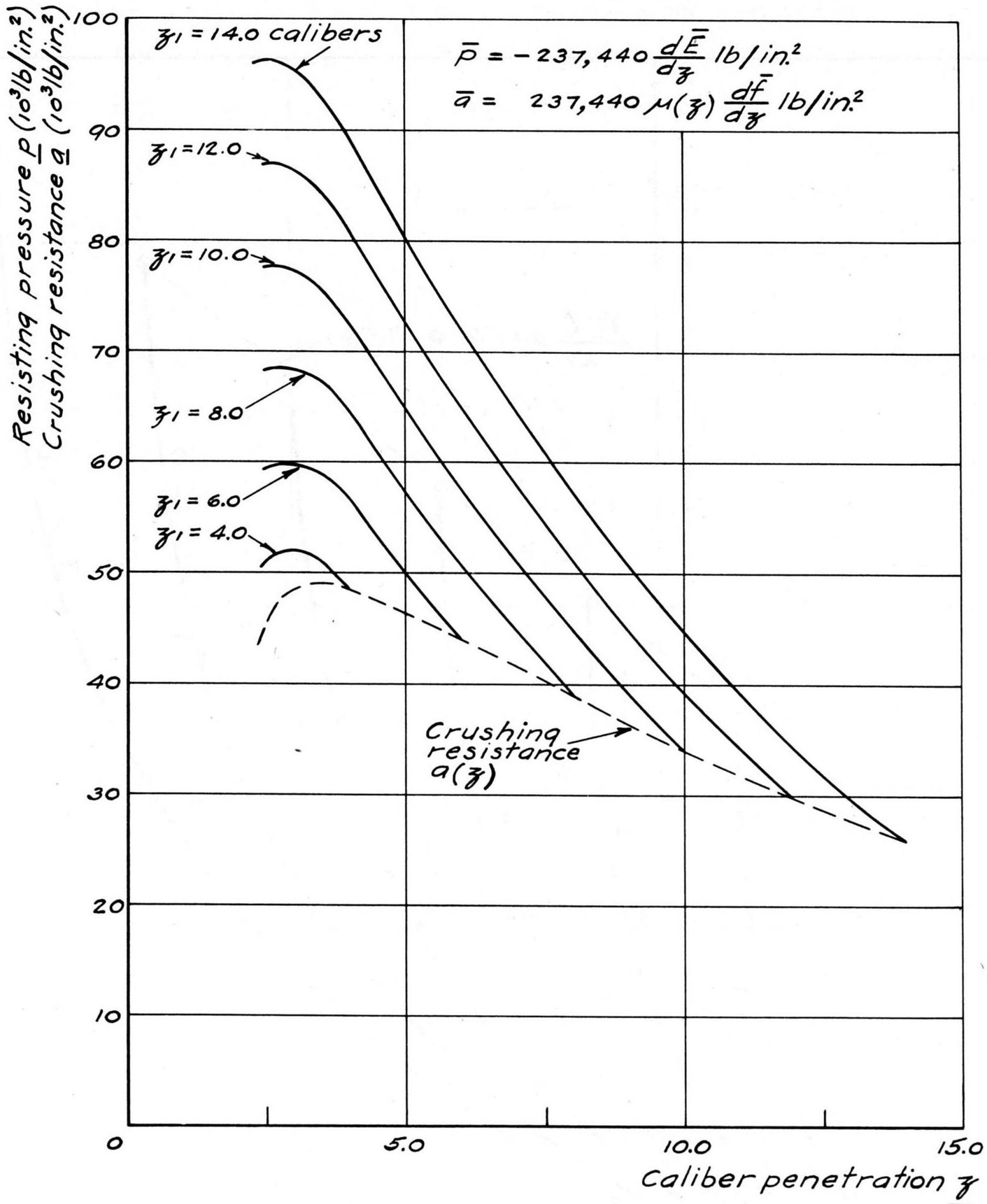

Fig. 10. Resisting pressure p (——) and crushing resistance q (– – –) versus instantaneous caliber penetration z during penetration.

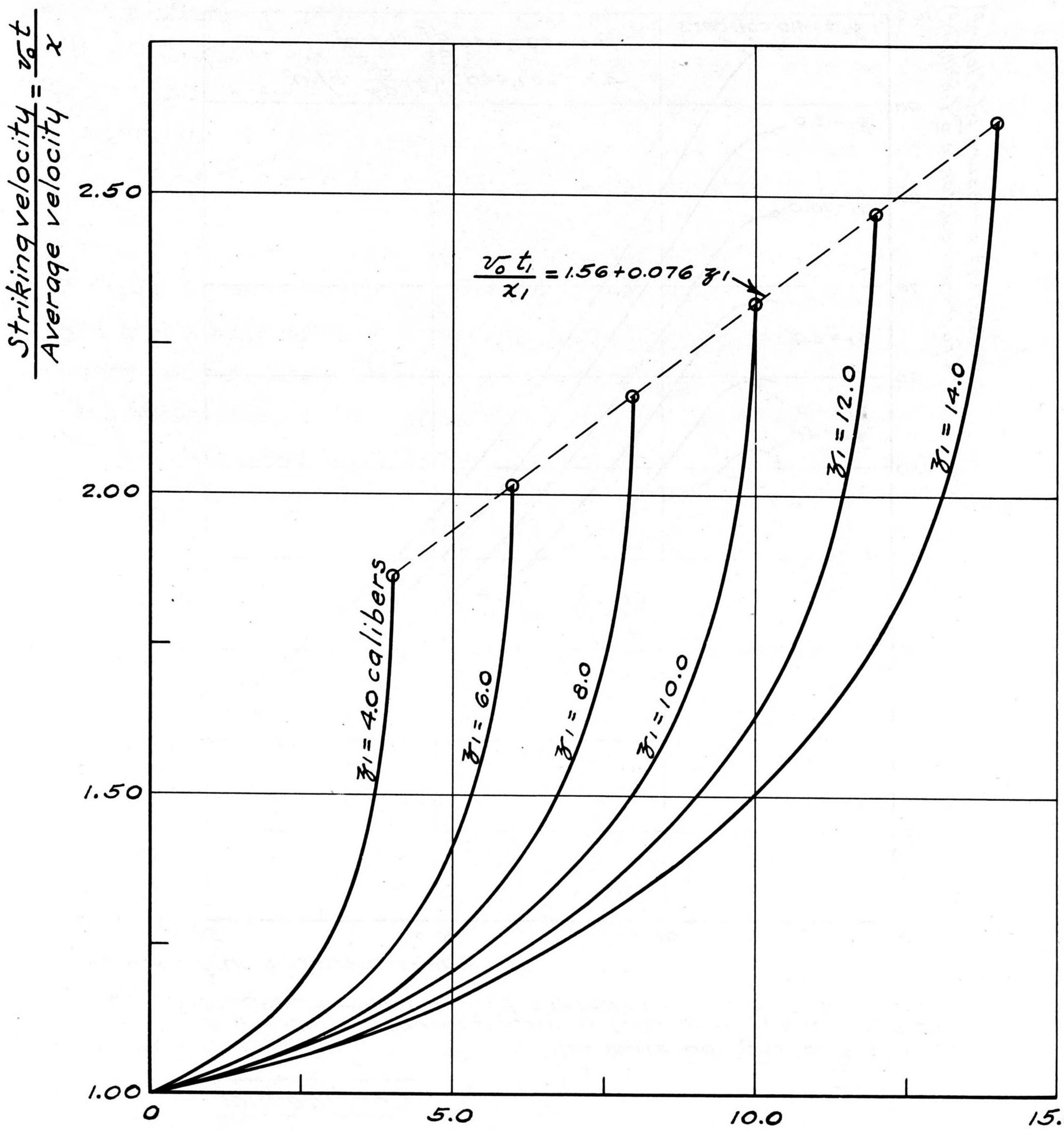

Fig. 11. Graph of $\frac{v_0 t}{x}$ as a function of z during penetration.

is particularly useful, especially when comparisons at different calibers are to be made; it may be regarded either as the ratio of the striking velocity v_o to the average velocity x/t to any point, or as the ratio of the distance that would have been covered in time t if the original striking velocity v_o had been maintained to the actual distance x covered in the target during this time. In the notation of Sec. II its value is

$$\frac{v_o t}{x} = \frac{\sqrt{E_o}}{z} \int_o^z \frac{dz}{\sqrt{E}}. \tag{34}$$

One may circumvent the awkwardness connected with the fact that E (see Fig. 9) in the denominator becomes zero for $z = z_1$ by using the following device in the numerical integration. If, for $z_a \leq z \leq z_b$, E is non-negative and (practically) a linear function of z, then it is easily shown that

$$\int_{z_a}^{z_b} \frac{dz}{\sqrt{E}} = \frac{2(z_b - z_a)}{\sqrt{E_a} + \sqrt{E_b}}. \tag{35}$$

The increments of Eq. (34) were computed numerically by this method.

As shown by the dashed straight line on the graph (Fig. 11), it is found that the computations for total time and maximum penetration can be expressed very well by the relation

$$\frac{v_o t_1}{x_1} = 1.56 + 0.076 z_1. \tag{36}$$

Until these calculations can be made for the actual calibers and caliber densities, it is felt that this relation may be used in selecting optimum fuze settings for HE bombs and projectiles. The curves of Fig. 11 show how insensitive the actual depth is to small errors in fuze time near the end of penetration.

VII. Summary and conclusions

An attempt has been made to establish a more satisfactory connection between penetration observations and a revised theory of penetration with a view to finding an improved formula of penetration and obtaining estimates of time, force, and velocity during penetration.

The lack of agreement between existing theories of penetration and the form of the observed penetration curve for a given combination of projectile and target is removed by the simple expedient of allowing the assumed force law to contain an undetermined function of depth x which is then evaluated from the observed penetration curve.

In the past, penetration formulas, both theoretical and empirical, have assumed that the ratio of depths reached by a given projectile with the same striking energy in different concretes is a constant, independent of the striking energy. Tests have shown this assumption to be inadequate.[19] The depth-dependence of the resisting force assumed in the present theory leads in a perfectly natural way to the result that the ratio of striking energies required by a given projectile to reach the same depth of penetration in different concretes should be a constant, independent of depth. This theoretical result gives an excellent representation of the observed facts.

Some new data on the effect of projectile nose shape on penetration are then analyzed by means of the same comparison principle and it is shown empirically that the ratio of striking energies required by otherwise similar projectiles of different nose shapes to reach a given depth of penetration is a constant, independent of penetration depth. These constant ratios, as evaluated from the data, seem to depend in a simple linear way on the length of the ogival noses of the projectiles.

Some new data on the effect of projectile mass on penetration are used to evaluate the remaining parameter in the assumed force law, namely the coefficient of the Poncelet-type inertia term. Three projectiles with relative masses of $\frac{2}{3}$:1:2 were used for the tests, and it is shown that the same value of the inertia coefficient results in a very satisfactory fit to the data for all three projectiles. The agreement is appreciably better than would be obtained either by making the customary assumption that the penetrations are proportional to projectile mass for each striking velocity, or by leaving out the inertia term in the assumed force law.

19/ See p. 22 in Ref. 9.

Having thus obtained a satisfactory representation of the dependence of penetration on striking velocity, target concrete, projectile nose shape, and projectile mass by means of the theory, sample calculations of velocity, resisting pressure, and time during penetration are carried out in Sec. VI by way of illustrating the scope of the relations that have been derived.

The results are felt to be sufficiently promising to warrant further work. The following points should be studied:

1. Only caliber .50 penetration data have been analyzed in terms of the proposed theory so far. Therefore, the most important next step would be to study the relation between penetration curves for different calibers on the same concrete; this amounts to a re-evaluation of the scale effect in terms of the new theory. One reason for elaborating the details of the further generalization of the theory in Appendix B is that they may be useful in finding a force law which will be consistent with penetration observations at all calibers. The data of the Penetration and Explosion Tests on Concrete Slabs[20] (P & E test) are particularly suitable since projectiles of different calibers were shot at the same slab at the same age in a number of cases. A preliminary check has shown that the average penetration curve for uncapped 37-mm projectiles on the largest P & E slabs is indistinguishable in shape from that given for caliber .50 E-6 projectiles (having almost the same caliber density) in Table I and Fig. 2 of the present report. For the other P & E calibers, namely 75-mm, 3-in., and 155-mm, an allowance will have to be made for their different caliber densities as outlined in Sec. V.

2. If the hoped-for common force law can be confirmed for all the calibers and caliber densities for which accurate data are available, then calculations like those in Sec. VI of velocity, force, and time during penetration should be made to cover the practical purposes for which these quantities are needed. In particular, the total time for maximum

---

20/ See Ref. 10.

penetration of HE bombs (large-caliber and low-caliber density) and anti-concrete HE projectiles should be estimated in order to specify optimum fuze times. The resisting force to which these missiles are subjected in concrete should likewise be evaluated in connection with problems of fuze-initiation and of rupture.

3. If, as in the case of caliber .50 projectiles, a considerable increase in the accuracy of estimating normal, nondeforming penetrations of all calibers results from the work of Item 1 above, then a comparison base will be available for a re-evaluation of existing data on oblique penetration, normal and oblique perforation, and residual velocity after perforation. These re-evaluations should be carried out with a view to making possible accurate and dependable predictions of these phenomena.

4. A re-evaluation should be made of the Concrete Properties Survey and similar data by computing the concrete factor for each of the concretes tested and studying its variation with various concrete properties. The improved accuracy of the "concrete factor" method may well lead to a clearer picture of the effect of various concrete properties on penetration resistance. This is of principal importance for the design of fortifications and other defensive structures, but should also aid in estimating the performance of our weapons against the types of concrete that the enemy is known to make and have. It would be very helpful to be able to express the concrete factor as a function of selected concrete properties and thus to include the effect of target in a general penetration formula. It remains to be seen whether anything better than the present rough approximations can be worked out for this purpose. Incidentally, since this analysis of the effect of concrete properties can be carried out quite independently of the scale-effect

investigation (Item 1 above), the results should give a fair test of the British assumption that the effect on penetration of aggregate size and of caliber should be completely representable in terms of their pure number ratio.

5. The same general method should be systematically applied to the problems of penetration in other materials, especially steel, armor, and soils. Even if the main problem of finding the law of force cannot be solved completely in each case, considerable improvements in the form of the empirical penetration formulas may be found that will enhance the accuracy and confidence with which extrapolatory predictions can be made.

APPENDIX A

An Experimental Method for Measuring Velocity as a Function of Time during Penetration

The most promising way of improving our understanding of penetration would be to obtain direct experimental observations of phenomena during penetration. Until these are obtained, theoretical considerations, such as those given in this report, will continue to be tentative and speculative. Even measurements of the total time of penetration alone would be most helpful.

The experimental work reported in Refs. 7 deals with an experimental method of measuring velocity as a function of time during penetration in nonmagnetic and nonconducting media like concrete. The basic ideas involved in this method are as follows.

The electromotive force induced by a longitudinally magnetized projectile (considered as a point dipole with a magnetic moment of M electromagnetic units) moving with a velocity v (cm/sec) along the axis of an idealized circular coil of N turns and r (cm) radius is

$$e = kvf(x) \text{ volts}, \tag{A-1}$$

where

$$k = \frac{6\pi MN}{10^8 r^2} \text{ volt-sec/cm}$$

and the "position function" $f(x)$, a pure number, is

$$f(x) = \frac{x}{(1 + x^2)^{5/2}}, \tag{A-2}$$

where x is the instantaneous position of the dipole on the coil axis measured in coil radii from the center of the coil. The position function $f(x)$ is plotted in Fig. A-1. In the absence of a resistant target, v is sensibly constant and x is proportional to the time t, measured from the instant $t = 0$ when the dipole is at the center of the coil. In this case Fig. A-1 is a picture of the form of the emf pulse as a function of time as commonly obtained from each coil in the solenoid method of measuring projectile velocities. If the projectile strikes a resistant target (nonmagnetic and nonconducting) placed near the coil, the emf pulse will be changed because v changes and because x is no longer proportional to t. On the assumption that the magnetic moment M does not materially change after impact it is in principle possible to deduce the projectile velocity as a function of time from an accurately recorded oscillographic trace of the emf pulse as a function of time.

A more direct determination of velocity as a function of time can be obtained by using two identical coaxial coils connected in opposition and spaced a distance of 0.90 diameters apart. Measuring x (in coil radii) from the point on the common axis midway between the coils, the induced electromotive force becomes

(A-3) $$e = kvF(x) \text{ volts},$$

where

(A-4) $$F(x) = f(x + 0.90) - f(x - 0.90).$$

This two-coil position function is shown in Fig. A-2 together with the two single-coil components of which it is composed. The flat-topped region of the graph illustrates the fact that

(A-5) $$F(x) = 0.4085 = \underline{\text{constant}}, \text{ within } \pm 1/3 \text{ percent}$$

while the dipole is in the interval

(A-6) $$-0.3 < x < 0.3$$

between the coils. Hence, <u>in this interval</u>, Eq. (A-3) becomes

(A-7) $$e = 0.4085 \text{ kv volts};$$

that is, the induced electromotive force is proportional to the projectile velocity at each instant and is <u>independent of x</u> to a very good approximation. The oscillograph trace will give directly the velocity as a function of time while the magnetic center of the projectile is in the interval (A-6); the target should therefore be placed so that the decelerations to be observed occur in this interval.

It is of some scientific interest to point out that this two-coil arrangement is very closely related to a two-coil arrangement specified by Maxwell[21/] for obtaining a nearly uniform magnetic field gradient near the axis midpoint. Maxwell's spacing between coils is $\sqrt{3}/2 = 0.866$ diameters; the 0.90-diameter spacing is a compromise which serves to extend the useful interval (A-6) somewhat without materially affecting the constancy of F(x) for practical purposes. The underlying connection between the present arrangement and Maxwell's becomes clear if we consider the dipole as moving in the magnetic field of a current flowing in the coils and equate the rate of work done on the dipole to the additional power required by the current to overcome the induced electromotive force.

The two-coil arrangement not only has the advantage over the single-coil system of greatly simplifying the routine analysis of the recorded

---

21/ See 715, pp. 358 to 359 in Vol. II, <u>Electricity and magnetism</u>, by J. C. Maxwell, 3rd ed. (Clarendon Press, Oxford, 1892).

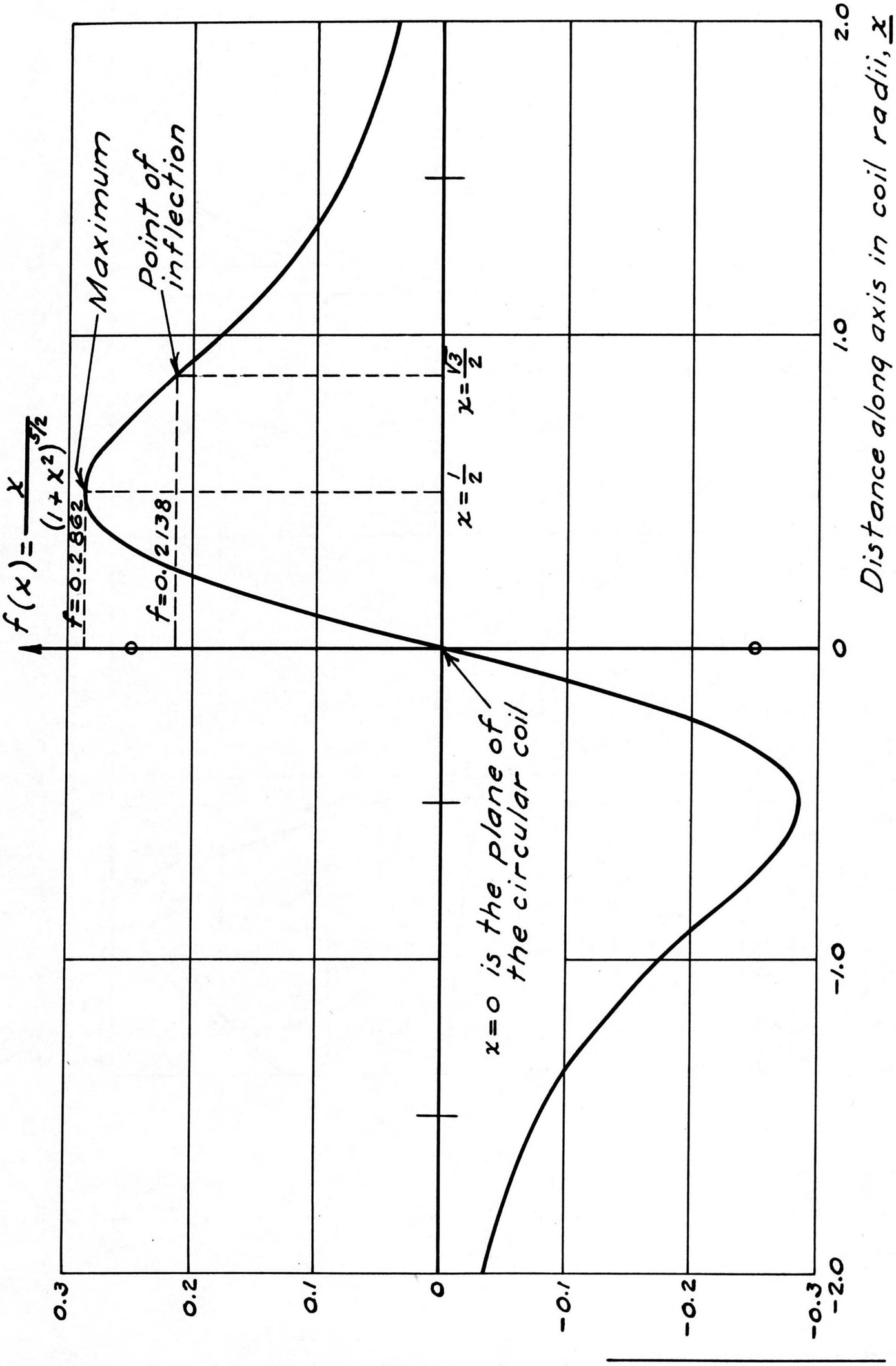

Fig. A-1. The position function f(x) for a single coil.

Confidential

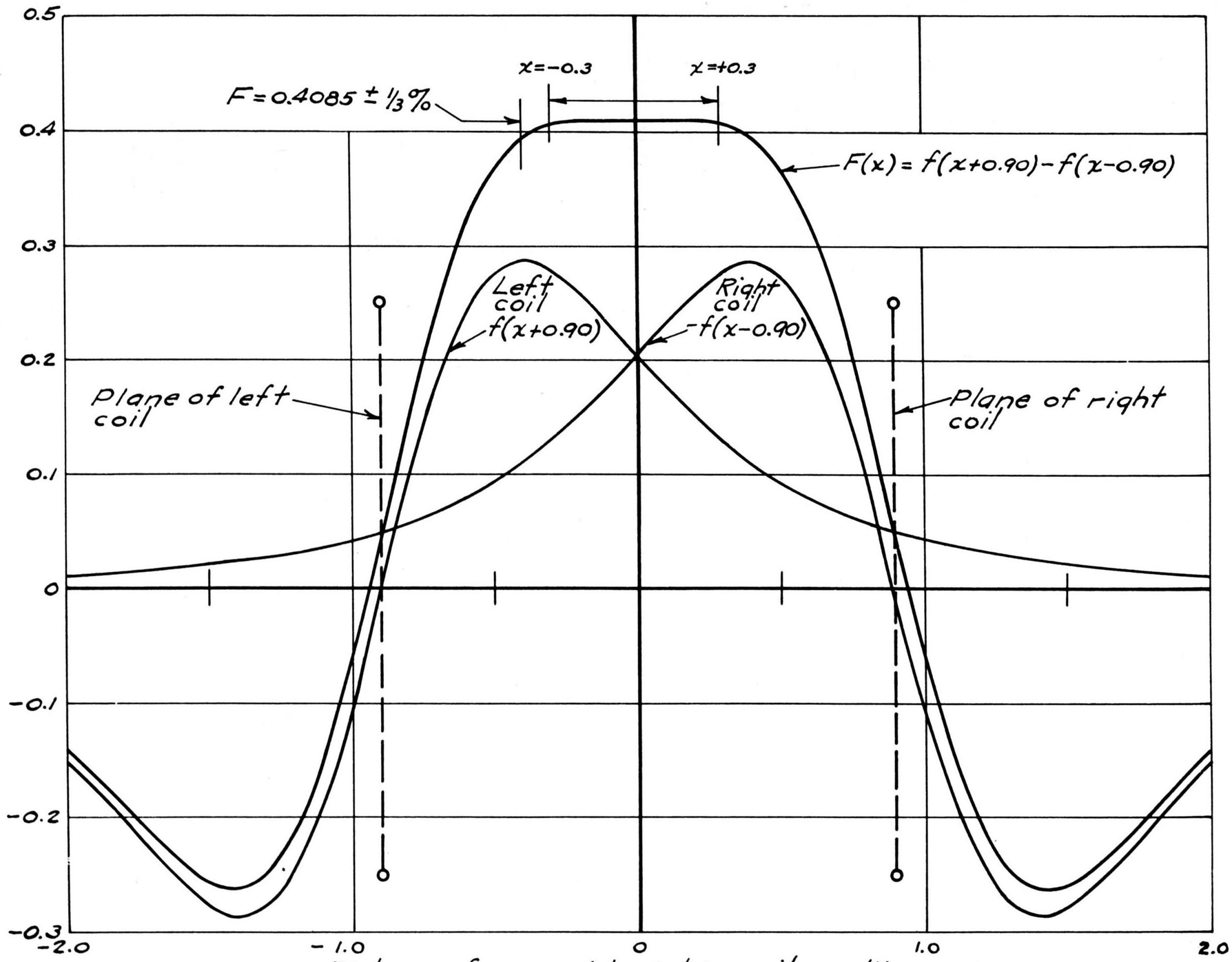

Fig. A-2. The position function F(x) for two opposing coils 0.90 diameters apart.

oscillograph traces, but it makes it easier to assess the accuracy of the resulting v(t)-curves and to recognize imperfections in the recording system which might otherwise lead to erroneous v(t)-curves.

References 7 deal with experimental work using the two-coil system, particularly the initiating and recording system and the problem of stabilizing the bullets to reduce the change in magnetic moment during impact to a minimum. Satisfactory performance was obtained with service caliber .50 AP bullets, and the problem of stabilizing experimental caliber .50 E-6 bullets had just been begun when the work was interrupted in order to transfer the available personnel to more important problems.

It seems probable that experimental information of considerable value in connection with the determination of the following quantities may be obtainable by the further development, adaptation, and exploitation of this method:

(1) Time as a function of depth during penetration and, in particular, time for maximum penetration for various missiles, striking conditions, and target strengths. This would be of use in specifying fuze settings of projectiles and bombs for maximum effect against concrete and similar materials.

(2) Resisting force as a function of time or depth during penetration for various striking velocities, nose shapes, target thicknesses and strengths. Such information would be of use in (a) specifying the minimum thickness of target necessary to initiate inertia-type fuzes, (b) specifying targets and striking conditions likely to cause deformation or rupture of HE bombs and projectiles against concrete, and (c) furnishing a basis for the design of HE missiles to secure maximum effect without rupture.

(3) Remaining velocity at various depths in a target and after perforation. It will be noted that the negative peaks before and after the flat-top in Fig. A-2 may be used as auxiliary measures or checks of striking and residual velocities, respectively. Such information would be of use in (a) studying the protective value of laminated or spaced slabs, (b) analyzing the maximum perforation of a bomb through successive concrete floors of a structure, and (c) finding the relation between striking and residual velocities for concrete and other slabs.

Whenever the determination of one or more of these quantities becomes sufficiently important to justify the use of scientific facilities and trained personnel it is recommended that the application of this method be considered in connection therewith.

APPENDIX B

A Further Generalization of the Poncelet Force Law

It is possible to integrate the equation of motion explicitly for the following further generalization of the Poncelet force law:

(B-1) $$\text{Resisting pressure} = p = a(x)v^{2\lambda} + b(x)v^2$$

For $\lambda = 0$ and $b(x) =$ constant, this reduces to the force law, Eq. (1), in Sec. II of this report. This assumption still belongs to the restricted class of force laws which depend only on $\underline{x}$ and $\underline{v}$. The first term on the right-hand side makes it possible to approximate an increase of crushing resistance with rate of strain (for example, v/d) by taking $\lambda > 0$, which would yield a "scale effect" dependence qualitatively in the right direction since $(v/d)^{2\lambda}$ would decrease with increase of $\underline{d}$; that is, the resisting pressure would be smaller for larger calibers. The difficulty that the resistance, Eq. (B-1), goes to zero as $\underline{v}$ becomes zero may not be serious for small values of $\underline{\lambda}$. In any case it would be possible to cut off the integrations at some value $v = v_c$ and take $\lambda = 0$ for $v_c \geq v \geq 0$ in order to improve the approximation.

It may also be that there is a variation of inertial resistance during penetration which could be approximated by allowing $b(x)$ to vary with depth in the target. Doubtless the effect of the target material displaced and accelerated at each point of the projectile's penetration is transmitted forward as well as sideways. The forward components would tend to reduce or change the values of the Poncelet $\underline{a}$ and $\underline{b}$ effective at later points of the penetration cycle. It seems very difficult to formulate these phenomena mathematically: the speed of propagation of elastic and plastic disturbances in the target material may be important and the resisting force may well depend on other variables beside $\underline{x}$ and $\underline{v}$; the underlying cause of the observed scale effect may be bound up with these difficulties. Nevertheless, the postulated $\underline{x}$ and $\underline{v}$ dependences may give a fair approximation to the resisting forces for the range of velocities and penetrations in which we are interested from the practical point of view. On the whole these speculations and uncertainties serve to emphasize once more the need for direct experimental observations of phenomena during penetration as discussed in Sec. I and Appendix A.

As in Eq. (2) of the text we introduce the dimensionless "inertia coefficient"

(B-2) $$\gamma(x) = \frac{2g}{w'} b(x),$$

which now depends on $\underline{x}$. The equation of motion is still a first-order linear differential equation in terms of the quantity

(B-3) $$U_\lambda = \frac{1}{1-\lambda} \cdot \frac{P}{2g} \cdot v^{2(1-\lambda)} = K U^{1-\lambda},$$

where

(B-4) $$K = \frac{1}{1-\lambda}\left(\frac{P}{2g}\right)^{\lambda}$$ (in particular, $K = 1$ for $\lambda = 0$)

and

$$U \equiv \frac{Pv^2}{2g} = \text{specific kinetic energy (as before).}$$

The equation of motion is then

(B-5) $$\frac{dU_\lambda}{dx} + (1-\lambda)\frac{w'}{P}\gamma(x)U_\lambda = -a(x).$$

Using the initial conditions, the solution is

(B-6) $$U_\lambda = \mu_\lambda(x)[U_{\lambda,o} - u_\lambda(x)],$$

where

(B-7) $$u_\lambda(x) = \int_o^x \frac{a(x)}{\mu_\lambda(x)}\,dx,$$

(B-8) $$\mu_\lambda(x) = [\mu(x)]^{1-\lambda},$$

(B-9) $$\mu(x) = e^{-\overline{\gamma}(x)w'x/P},$$

and $\overline{\gamma}(x)$ is the "mean inertia coefficient," a pure number, equal to the mean value of $\gamma(x)$ from 0 to $\underline{x}$. The quantity $\overline{\gamma}(x)$ is thus

(B-10) $$\overline{\gamma}(x) = \frac{1}{x}\int_o^x \gamma(x)\,dx.$$

The function $\mu(x)$, which does not depend on $\underline{\lambda}$, has been introduced to facilitate working out the relationship between these formulas and the observed penetration curve; for the latter we maintain the notation of Eq. (8), Sec. II, namely

(B-11) $$U_o = u(x_1).$$

Inserting the final conditions at the end of penetration in Eq. (B-6) and noting Eq. (B-3), we obtain

(B-12) $$U_{\lambda,o} = u_\lambda(x_1) = KU_o^{1-\lambda} = K[u(x_1)]^{1-\lambda}.$$

Thus the function $u_\lambda(x)$ is obtainable from the observed $u(x)$ for any $\underline{\lambda}$:

$$u_\lambda(x) = K[u(x)]^{1-\lambda}. \tag{B-13}$$

Inserting Eqs. (B-3), (B-8), (B-12), and (B-13) in the integral (B-6) we have, after simplifying,

$$U = \mu(x)\left\{U_o^{1-\lambda} - [u(x)]^{1-\lambda}\right\}^{\frac{1}{1-\lambda}}. \tag{B-14}$$

Thus the remaining specific kinetic energy $\underline{U}$ at each point $\underline{x}$ during penetration can be computed from the striking energy U_o, the penetration curve $u(x)$, the mean inertia coefficient $\overline{\gamma}(x)$, and the parameter $\underline{\lambda}$. It follows that, using Eq. (B-14) instead of Eq. (6), the instantaneous values of the resisting pressure $\underline{p}$, the velocity $\underline{v}$, and the time $\underline{t}$ are given by the same equations as before, namely Eqs. (9), (10), and (11), respectively, of Sec. II. It is noteworthy that an explicit knowledge of $a(x)$ is not required for these computations of $\underline{p}$, $\underline{v}$, and $\underline{t}$ during penetration.

If by some means (for example, scale-effect data) $\underline{\lambda}$ can be evaluated, then both $\overline{\gamma}(x)$ and $a(x)$ can, in principle, be calculated as follows from penetration curves, $u_\alpha(x)$ and $u_\beta(x)$, observed with sufficient accuracy for two projectiles of different masses (sectional pressures P_α and P_β) but of the same shape and caliber on the same concrete. From Eq. (B-13) we compute for each projectile the function

$$L(x) = \log_e \frac{du_\lambda(x)}{dx}. \tag{B-15}$$

It follows from Eqs. (B-7), (B-8), and (B-9) that

$$L_\alpha(x) = \log_e a(x) + (1 - \lambda)\,\overline{\gamma}(x)\,\frac{w'}{P_\alpha}\,x,$$

and similarly for $L_\beta(x)$. The solution of these simultaneous equations yields the required relations:

$$\log_e a(x) = \frac{P_\alpha L_\alpha(x) - P_\beta L_\beta(x)}{P_\alpha - P_\beta}, \tag{B-16}$$

$$\overline{\gamma}(x) = \frac{1}{(1 - \lambda)\,w'x} \cdot \frac{L_\alpha(x) - L_\beta(x)}{\frac{1}{P_\alpha} - \frac{1}{P_\beta}}, \tag{B-17}$$

which depend on $\underline{\lambda}$ through Eq. (B-15).

The calculations for $\underline{p}$, $\underline{v}$, $\underline{t}$, and, particularly, the evaluation of $\overline{\gamma}(x)$ depend on the accuracy of our knowledge of the penetration curves $u(x)$. As in Sec. III we can derive averaging methods to enhance the precision of the observed curves. We introduce the following appropriately

revised but equally plausible "supplementary assumption" into the generalized theory:

> For a group of similar concrete targets the crushing-resistance coefficients a(x) in Eq. (B-1) bear constant ratios to one another for all values of $\underline{x}$.

Thus each a(x) is proportional to some standard function $a_s(x)$ which is the same for all targets of the group:

$$a(x) = C_\lambda a_s(x). \tag{B-18}$$

It follows from Eq. (B-7) that

$$u_\lambda(x) = C_\lambda u_{\lambda,s}(x), \tag{B-19}$$

and from Eq. (B-13) that

$$u(x) = C_\lambda^{1/(1-\lambda)} u_s(x). \tag{B-20}$$

The generalized theory thus leads to exactly the same method of comparing and averaging penetration curves as the restricted theory did in Sec. III. In fact, we are free to identify $u_s(x)$ with the average penetration curve $\bar{u}(x)$ for the group and to write, as in Eq. (23) of Sec. III,

$$u(x) = C\bar{u}(x), \tag{B-21}$$

where the concrete factor

$$C = C_\lambda^{1/(1-\lambda)} \tag{B-22}$$

is the same, quite independent of $\underline{\lambda}$, as that defined in Sec. III.

These considerations lead to the unexpected and striking conclusion that any success of the restricted theory of the text in relating the penetration curves for the same projectile on different concretes not only does not constitute evidence against the generalized theory but actually gives equal support for the latter!

APPENDIX C

Penetration Data on Caliber .50 Special Projectiles

The Princeton Concrete Properties Survey (CPS) was an experimental study of the effect of concrete properties on penetration resistance;[22] for this purpose the same projectile (caliber .50 E-6 projectile) was used in testing the penetration resistance of a large number of different concretes. In order to obtain some data on the effect of different projectile masses and shapes on penetration, the series of tests here reported were made during the work of the CPS, utilizing the same methods and equipment.

The various special caliber .50 projectiles are shown in Fig. C-1. Three solenoids were used with the chronograph for measuring the velocities as previously described,[23] and the instrumental velocities were corrected for the velocity decrease over the distance (about 13, 18, and 23 ft, respectively, for the various solenoid combinations used) to the target cube. Different form factors $\underline{i}$ and G-tables are required for the different projectiles, and we wish to thank H. P. Hitchcock and R. W. Ladenburg of the Ballistic Research Laboratory, Aberdeen Proving Ground, for their help and advice in deciding upon the values used. The velocity corrections were made according to the equation,

$$\Delta v = -\underline{i}G \frac{d^2}{w} \Delta x, \tag{C-1}$$

where

Δv (ft/sec) = velocity correction,
d (in.) = projectile diameter,
w (lb) = projectile weight,
Δx (ft) = distance from midpoint of solenoid interval to target.

The values of the product $\underline{iG}$ for the various projectiles were read from the curves of Fig. C-2.

The mix design and concrete properties of the targets are given in Table C-I. The cubes were made in sets of five, one cube from each of five batches mixed and poured identically on the same day. Test cylinders and beams were made from each batch. In the analysis of the penetration data it is assumed that there was no significant variation in the concrete of different cubes made on the same day and that average values of the measured concrete strengths apply to all five targets. All cubes were reinforced as described in Ref. 9 with the exception of the last set, cubes

---

22/ See Ref. 9.

23/ See pp. B-3 and B-4 in Appendix B of Ref. 9.

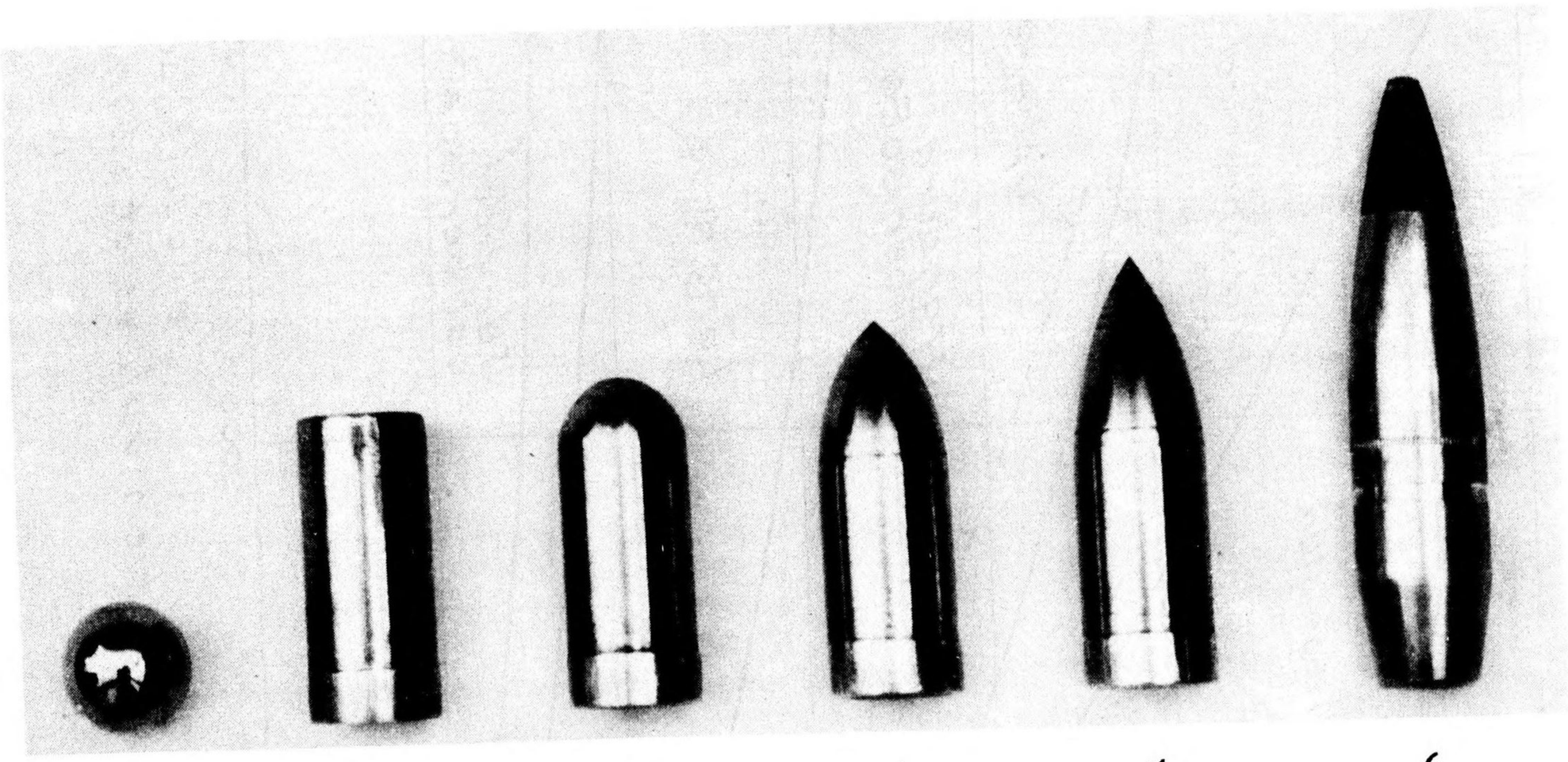

1 2 3 4 5 6

No.	Type Projectile		Caliber Radius Ogive = n	
1	Spherical ($\frac{1}{2}$-in. ball bearing)		0.50	d = 0.4985 ± 0.0010 in.
2	Flat-nosed slug		----	
3	Hemispherical-nosed		0.50	
4	Hollow Standard Tungsten carbide	E-6	1.50	
5	Long-nosed		3.10	
6	Service AP		----	

Fig. C-1. Caliber .50 special projectiles.

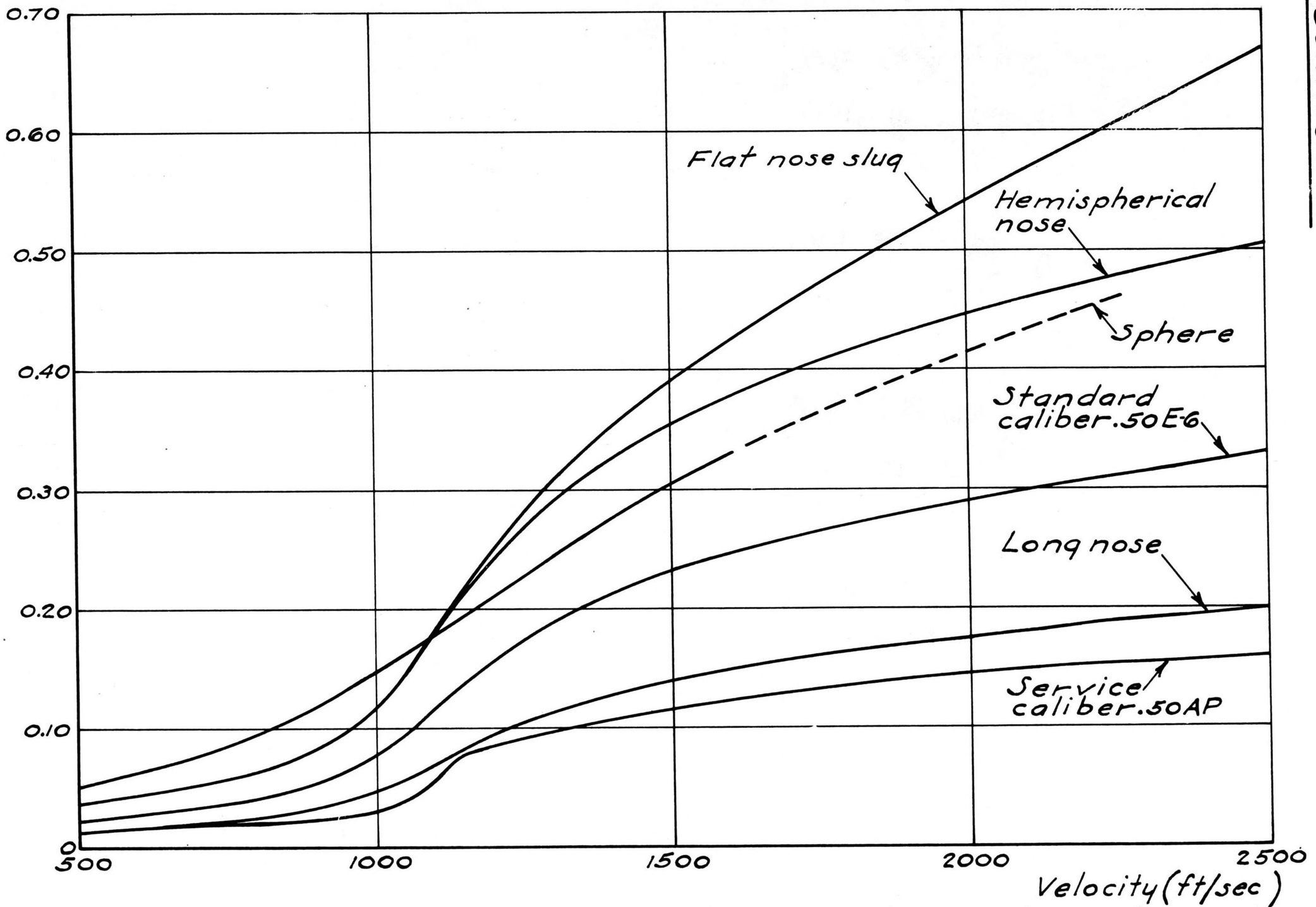

Fig. C-2. Special projectiles: Velocity correction values of iG in the formula $\Delta v = -iG \frac{w}{d^2} \Delta x$.

Confidential

B3B 25-29. The latter were made without the reinforcing "cage" so that they could be broken apart to measure the maximum core penetration of the service AP bullets. Unless this is done the usual depth-gauge measurement by probing may inadvertently be made to a part of the jacket, which usually lodges in the hole at varying distances behind the core.

The penetration data are given in Tables C-II to C-VI. The measuring and recording procedures are described in detail in Appendix B of Ref. 9. All cubes were tested for penetration after aging 28 days. The average compressive strength S_c (lb/in^2) was measured on 4 × 8-in. cylinders fog-cured with the cubes for 28 days. If the bullet stuck, the penetration given is the measurement to the center of the base of the bullet plus the length of the bullet unless otherwise noted in the "Remarks" column: the value may be too small if the bullet rebounded in the hole; furthermore, sticking is significant for full-scale explosive projectiles. For these reasons sticking has always been noted in Princeton tests. The top and bottom faces of these cubes as poured were not tested for reasons previously discussed.[24]

24/ See p. 5 in Ref. 9.

CONFIDENTIAL

Table C-I. Mix quantities and physical properties of concrete*; 28-day fog-cured.

Normal cement Brand A of water-cement ratio 0.58 by weight
Quartz aggregate: 3/8-in. maximum size, gradation No. 14*
Design volumes: water, 20.5%; cement, 11.2%; aggregate, 68.3%

Batch and Target No.	Aggregate Fineness Modulus	Slump (in.)	Specific Gravity		Curing Absorption (% of volume)		Voids (% of volume)			Compressive Strength (lb/in²)		Flexural Strength (lb/in²)	Modulus of Elasticity (10^6 lb/in²)
							Air		Air-Water	4 × 8-in. Cylinder	Modified Cube		
			Cube	Cylinder	Cube	Cylinder	Cube	Cylinder	Cylinder				
B3B 3	3.97	3/4	2.30	2.35	0.4	0.8	2.6	0.5	--	4480	4380	750	5.47
B3B 4	3.97	1/2	2.31	2.34	.8	.8	2.4	.7	16.0	4450	--	--	--
B3B 5	3.97	3/4	2.32	2.35	.3	.8	1.9	.5	--	4410	4210	750	5.47
B3B 6	3.97	1/2	2.32	2.35	1.6	.7	2.2	.6	15.8	4480	--	--	--
B3B 7	3.97	3/4	2.31	2.34	1.0	.8	2.5	.8	--	4410	4230	755	5.33
B3B 8	3.97	1-3/8	2.31	2.34	0.8	1.2	1.9	1.0	--	4300	4060	735	5.43
B3B 9	3.97	1-1/4	2.31	2.33	1.2	1.2	2.3	1.4	17.4	4180	--	--	--
B3B 10	3.97	1-1/2	2.32	2.33	1.4	1.4	1.8	1.5	--	4250	4510	750	5.37
B3B 11	3.97	1-1/4	2.31	2.32	2.2	1.4	2.5	1.7	17.1	4260	--	--	--
B3B 12	3.97	1-3/8	2.31	2.32	1.7	1.3	2.5	1.7	--	4200	4190	830	5.40
B3B 13	4.07	1-1/4	2.31	2.33	0.9	0.9	1.8	1.3	--	4120	4170	680	5.29
B3B 14	4.07	1-5/8	2.32	2.32	.9	0.9	1.5	1.5	17.0	3930	--	--	--
B3B 15	4.07	1-1/4	2.31	2.33	.5	1.1	1.6	1.3	--	4010	4300	730	5.36
B3B 16	4.07	1-3/8	2.32	2.32	.2	1.1	1.3	1.6	17.1	4140	--	--	--
B3B 17	4.07	1-1/2	2.33	2.33	.2	1.0	1.0	1.2	--	4100	4130	725	5.29
B3B 20	4.03	1-1/4	2.33	2.28	1.1	1.0	1.4	3.4	19.3	3800	4860	830	5.32
B3B 21	4.03	1-1/8	2.33	2.31	1.5	0.9	1.8	2.2	18.2	3890	--	--	--
B3B 22	4.03	1-1/8	2.32	2.30	1.7	1.0	2.0	2.6	17.4	3560	4870	825	5.30
B3B 23	4.03	1-1/8	2.32	2.30	0.9	1.1	1.9	2.6	18.0	3700	--	--	--
B3B 24	4.03	1	2.31	2.29	1.0	1.1	2.3	3.4	--	3830	4620	790	5.29
B3B 25	4.09	1-5/8	2.35	2.30	0.1	0.8	0.1	2.7	--	3700	4770	810	5.33
B3B 26	4.09	1-1/2	2.34	2.29	0.5	1.0	.8	3.1	18.6	3490	4680	840	5.22
B3B 27	4.09	1-3/4	2.35	2.30	1.1	0.9	.5	2.8	17.6	4030	4790	790	5.30
B3B 28	4.09	1-1/2	2.34	2.28	0.8	0.9	1.0	3.3	18.5	3880	4680	840	5.22
B3B 29	4.09	1-5/8	2.35	2.30	0.9	1.0	0.6	2.7	18.7	3780	4730	820	5.29

*Methods of measurement and terminology are the same as in Ref. 9. Compare Table II and Table A-VI (Appendix A) of Ref. 9.

Table C-II. Effect of nose shape on penetration in concrete:

Comparative performance of standard E-6 and flat-nosed caliber .50 special projectiles.

Targets: Cubes B3B 3 to B3B 7; average compressive strength, 4445 lb/in²

Round No.	B3B Cube No.	Mass of Bullet (gm)	Striking Velocity[a] (ft/sec)	Nose Penetration[a] (in²)	Crater Size		Remarks
					Depth (in.)	Radius (in.)	
Standard E-6 projectile: average mass, 29.31 gm; average caliber density D, 0.5215 lb/in³							
534	7	29.41	574	0.81±	0.7	1.3	Yaw 45°?
516	3	29.16	743	1.02	1.0	1.3	
520	4	29.28	945	1.40	1.15	2.1	
530	6	29.23	971	1.42	1.1	1.9	
526	5	29.32	1138	1.87	1.2	2.7	
517	3	29.20	1583	*2.86	1.1	2.4	Bullet at 20°.
535	7	29.29	1706	*3.01	1.2	1.9	Bullet at 7°.
521	4	29.34	1823	*3.46	1.2	3.2	
527	5	29.37	2076	*4.31	1.1	2.0	Path at 10°.
531	6	29.51	2237	*4.82	1.3	2.4	
Flat-nosed projectile:[b] average mass, 28.36 gm; average caliber density D, 0.5046 lb/in³							
518	3	28.31	735	0.85	0.80	1.2	
532	7	28.33	823	0.95	0.95	1.6	
522	4	28.50	876±	1.07	1.05	1.4	
524	5	28.44	1096	1.30±	1.30	2.1	Flat aggregate imprint at 1.21 in.
528	6	28.35	1325	1.66	1.65	2.6	Partial flat imprint.
519	3	28.33	1603	*2.20	1.40	2.5	
533	7	28.24	1759	*2.43	1.55	2.1	
523	4	28.30	1837	*2.44	1.55	2.7	
525	5	28.45	2037	*2.99	1.60	2.1	
529	6	28.32	2244	*3.65	1.40	2.4	Band off. Stuck behind bullet.

a/ The symbol ± means that the measurement is felt to be less accurate than other like measurements.

The symbol * before a penetration value means that the bullet stuck and that the penetration given is the measurement to the center of the base of the bullet plus the length of the bullet unless otherwise noted in the "Remarks" column.

b/ As a rule flat-nosed projectiles did not leave a definite nose impression.

Table C-III. Effect of mass on penetration in concrete:

Comparative performance of standard E-6, hollow E-6, and tungsten carbide E-6 caliber .50 special projectiles.

Targets: Cubes B3B 8 to B3B 12; average compressive strength, 4240 lb/in.^{2}

Round No.	B3B Cube No.	Mass of Bullet (gm)	Striking Velocity[a] (ft/sec)	Nose Penetration[a] (in.)	Crater Size		Remarks
					Depth (in.)	Radius (in.)	
Standard E-6 projectile: average mass, 29.07 gm; average caliber density D, 0.5172 lb/in.^{3}							
552	11	29.13	1207	*1.97	1.35	2.0	Bullet at angle. Removed.
555	10	29.18	1303	*2.35	1.2	2.2	Bullet removed for measuring.
560	12	29.23	1313	*2.19±	1.15	2.4	Removed. x = 2.45 in. at 30°
554	10	28.63	1603	*2.96	1.2	3.4	
558	12	29.18	1858	*3.86	1.1	2.0	
Hollow E-6 projectile: average mass, 20.28 gm; average caliber density D, 0.3608 lb/in.^{3}							
537	8	20.18	1492	*1.95	1.18	3.7	Bullet at 15°. Removed.
545	9	20.28	1530	2.10	1.60	2.4	
547	9	20.55	1715	*2.44	0.99	2.7	
540	8	20.12	1783	*2.59	1.10	2.7	
Tungsten carbide E-6 projectile: average mass, 58.70 gm; average caliber density D, 1.0445 lb/in.^{3}							
546	9	58.76	794±	1.85	1.55	1.8	Yaw 20°?
556	10	58.64	919	*2.51	0.90	2.3	Bullet removed for measuring.
542	9	58.95	1012	*2.72	1.05	2.1	Base broken. Removed.
559	12	58.68	1087	*3.25±	1.20	2.1	Bullet base broken.
557	12	58.39	1137	*3.22±	1.05	2.6	Bullet at 15°. Base broken.
541	8	58.69	1309	*4.70±	1.28	2.9	Bullet base shattered.
551	11	58.87	1463	*5.60±	1.30	2.6	Bullet base chipped.
538	8	58.65	1489	*5.52	0.89	3.7	

a/ The symbol ± means that the measurement is felt to be less accurate than other like measurements.

The symbol * before a penetration value means that the bullet stuck and that the penetration given is the measurement to the center of the base of the bullet plus the length of the bullet unless otherwise noted in the "Remarks" column.

Table C-IV. Effect of nose shape on penetration in concrete:

Comparative performance of standard E-6, hemispherical-nosed, and flat-nosed caliber .50 special projectiles.

Target: Cubes B3B 13 to B3B 17; average compressive strength, 4060 lb/in.^{2}

Round No.	B3B Cube No.	Mass of Bullet (gm)	Striking Velocity (ft/sec)	Nose Penetration[a] (in.)	Crater Size		Remarks
					Depth (in.)	Radius (in.)	
Standard E-6 projectile: average mass, 29.05 gm; average caliber density D, 0.5169 lb/in.^{3}							
561	13	29.20	775	1.22	0.95	1.3	
576	16	29.17	973	1.53	1.25	1.9	
580	17	28.64	1155	*1.99	1.12	2.3	Slight angle. Removed.
564	13	29.05	1418	*2.28	1.30	1.7	Bullet at 15°. Removed.
567	14	29.01	1436	*2.54	1.20	2.6	Bullet at small angle.
570	15	29.03	1652	*3.25	1.32	2.3	Bullet at slight angle.
573	16	29.28	2178	*5.16	1.25	2.8	Bullet at 10°.
Hemispherical-nosed projectile: average mass, 28.07 gm; average caliber density D, 0.4995 lb/in.^{3}							
562	13	27.92	825	1.09	0.90	1.3	
565	14	28.10	1312	*2.00	1.00	1.8	Bullet removed for measuring.
578	17	27.92	1323	*2.13	1.18	2.5	Bullet at 10°. Removed.
568	14	28.34	1401	*2.16	1.20	2.5	Bullet at 10°. Removed.
574	16	27.99	1431	*2.36	1.25	2.8	Bullet at 5°. Removed.
571	15	28.14	1630	*2.62	1.59	2.9	Bullet removed for measuring.
577	17	28.09	1985	*4.09	1.28	2.8	
Flat-nosed projectile: average mass, 28.31 gm; average caliber density D, 0.5037 lb/in.^{3}							
563	13	28.34	868	1.06	1.06	1.5	
566	14	28.35	1156	1.51	1.12	2.5	
569	15	28.45	1579	*2.10	1.45	2.8	Bullet removed for measuring.
572	15	28.29	1604	*2.20	1.34	1.9	Bullet at 10°. Removed.
575	16	28.23	1728	*2.81	1.50	2.6	
579	17	28.22	1941	*3.12	1.58	2.9	Bullet removed for measuring.

a/ The symbol * before a penetration value means that the bullet stuck and that the penetration given is the measurement to the center of the base of the bullet plus the length of the bullet unless otherwise noted in the "Remarks" column.

Table C-V. Effect of nose shape and mass on penetration in concrete:

Comparative performance of caliber .50 special projectiles: standard E-6, long-nosed, and spheres.

Target: Cubes B3B 20 to B3B 24; average compressive strength, 3755 lb/in.^{2}

Round No.	B3B Cube No.	Mass of Bullet (gm)	Striking Velocity (ft/sec)	Nose Penetration[a] (in.)	Crater Size		Remarks
					Depth (in.)	Radius (in.)	
Standard E-6 projectile: average mass, 28.85 gm; average caliber density D, 0.5133 lb/in.^{3}							
865	23	28.58	672	0.90±	0.72	1.9	Imprint at 30°.
862	23	28.65	853	1.26	0.95	1.9	Imprint at 10°.
868	20	28.96	1122	1.56±	1.11	2.7	Imprint at 40°.
871	21	28.93	1385	2.18	1.56	2.5	Imprint at 10°.
874	22	29.12	1675	*2.83	1.20	3.5	Stuck at 25°.
877	22	28.85	1865	*3.32	1.71	2.9±	
Long-nosed projectile: average mass, 30.54 gm; average caliber density D, 0.5434 lb/in.^{3}							
867	20	30.05	434	0.70±	0.51	0.9	Imprint at 45°.
864	23	30.60	759	1.27	0.92	1.9	
870	21	30.81	1114	1.80	1.35	1.9	Imprint at 15°.
873	21	30.55	1383	*2.45	1.12	2.6	
876	22	30.61	1669	*3.31	1.52	3.3	Bullet at 20°.
879	24	30.36	1890	*4.06±	1.50	4.4	Bullet at 45°.
881	24	30.80	2093	*4.60	1.40	3.9	
Spheres: average mass, 8.25 gm; average caliber density D, 0.146 lb/in.^{3}							
866	20	8.25	636	0.27	0.27	0.6	
863	23	8.25	823	.33	.42	1.0	
869	20	8.25	1315	.65	.67	1.6	
875	22	8.25	1594	.95	.84	1.7	
872	21	8.25	1583	.84	.85	1.5	
878	24	8.25	1863	1.08	1.02	1.9	
880	24	8.25	2236	1.40	1.23	2.3	

a/ The symbol ± means that the measurement is felt to be less accurate than other like measurements.

The symbol * before a penetration value means that the bullet stuck and that the penetration given is the measurement to the center of the base of the bullet plus the length of the bullet unless otherwise noted in the "Remarks" column.

Table C-VI. Effect of type of projectile on penetration in concrete:

Comparative performance of standard E-6 and service AP caliber .50 projectiles.

Target: Cubes B3B 25 to B3B 29, not reinforced; average compressive strength, 3775 lb/in.^{2}

Round No.	B3B Cube No.	Mass of Bullet (gm)	Striking Velocity (ft/sec)	Nose Penetration[a] (in.)	Crater Size		Remarks
					Depth (in.)	Radius (in.)	
Standard E-6 projectile: average mass, 29.02 gm; average caliber density D, 0.5164 lb/in.^{3}							
896	28	29.01	630	0.82±	0.70	1.3	Imprint at 30°.
890	27	28.43	893	1.20±	1.00	1.5	Imprint at 25°.
883	26	29.50	1203	1.90	1.35	1.8	Imprint at 20°.
897	28	29.00	1574	2.76	1.52	2.8±	
900	28	29.15	2330	4.9±	--	--	Cube demolished.
Service AP projectile: average mass, 45.58 gm; average caliber density D, 0.811 lb/in.^{3}							
888	27	45.63	672	0.96±	0.78	2.0	Imprint at 45°.
894	29	45.50	735	1.29±	.84	1.6	Imprint at 25°.
901	25	45.50	780	1.29	.90	1.9	Imprint at 20°.
892	29	45.60	1007	1.84	1.30	2.0	
893	29	45.60	1056	1.97	1.32	2.7	Imprint at 10°.
889	27	45.63	1263	*2.57±	1.23	3.5	Bullet at 35°.
884	26	45.50	1593	*3.43±	2.60	3.9	Bullet at 10°.
891	27	45.50	1676	*3.90	1.58	1.5	Path at 5°.
895	29	45.73	2285	6.70	--	--	Cube demolished.

a/ The symbol ± means that the measurement is felt to be less accurate than other like measurements.

The symbol * before a penetration value means that the bullet stuck and that the penetration given is the measurement to the center of the base of the bullet plus the length of the bullet unless otherwise noted in the "Remarks" column.

LIST OF REFERENCES

1. "Terminal ballistics I," by H. P. Robertson, Committee on Passive Protection Against Bombing. Interim Report, Jan. 1941. Unclassified

2. "Penetration of projectiles in concrete," by Richard A. Beth, Committee on Passive Protection Against Bombing. Interim Report No. 3, Nov. 1941. (Confidential)

3. "A brief summary of recent data on penetration in concrete at various scales," by R. A. Beth, Committee on Passive Protection Against Bombing. Interim Report No. 18, June 1942. (Confidential)

4. "Seventeenth interim report on concrete for defense works -- The effect of sectional density on the penetration into concrete of armour-piercing shot and the derivation of a general penetration formula." MOS 311/ACW, Feb. 1944. (British Secret)

5. "Penetration of reinforced concrete by AP projectiles and AP and SAP bombs," Weapon Data, Division 2, NDRC, Data Sheet 2A1, June 1943. (Confidential)

6. "Penetration theory: Estimates of velocity and time during penetration," by R. A. Beth. Issued as a contractor's informal memorandum in Mar. 1944; a revision with minor alterations appears in OTB-7 (OSRD-4720), p. 1. (Confidential)

7. "Progress of velocity-time program," by E. J. Schaefer. Issued as a contractor's informal memorandum Mar. and Apr. 1944; to be issued shortly as a formal NDRC memorandum of Division 2. (Confidential)

8. "Final Report to the Corps of Engineers, U.S. Army, for the year ending June 30, 1941, Part I," Committee on Passive Protection Against Bombing. July 1941. (Confidential)

9. "Effect of concrete properties on penetration resistance," Interim Report No. 27, Concrete Properties Survey, including Appendix A and Appendix B. July 1944. (Confidential)

10. "Penetration and explosion tests on concrete slabs. Report I: Data," by Richard A. Beth and J. Gordon Stipe, Jr., Committee on Passive Protection Against Bombing. Interim Report No. 20, Jan. 1943. (Confidential)

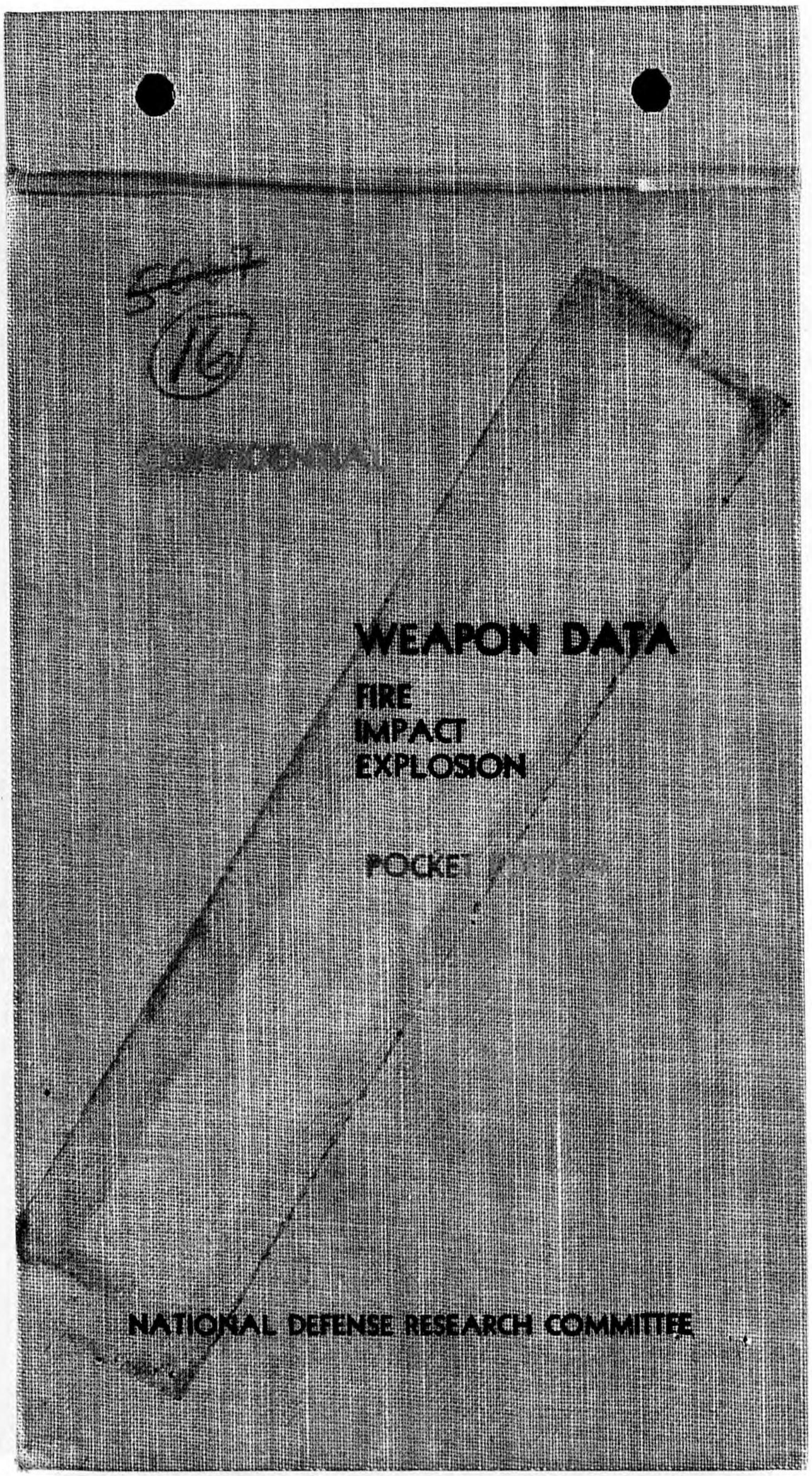
Sept
(6)
CONFIDENTIAL
WEAPON DATA
FIRE
IMPACT
EXPLOSION
POCKET
NATIONAL DEFENSE RESEARCH COMMITTEE

HEADQUARTERS ARMY AIR FORCES

ROUTING AND RECORD SHEET

CONFIDENTIAL

TALLY NO.	
FILE NO.	319.1

SUBJECT: NDRC Report, "Weapon Data: Fire, Impact, Explosion"

TO: Twentieth Air Force
Room 3E 1070, The Pentagon
Attn: A-3 Combat Operations - Colonel Combs

FROM: AC/AS, Materiel & Services, Air Ordnance Office

DATE 9 MAR 945

COMMENT No. 1

LB-bm 72343

Chief of Staff	
Deputy C. of S.	
Deputy C. of S. Opr.	
Deputy C. of S. T.M.&E.	
A. G.	

1. Attached hereto for your information is a pocket sized edition of NDRC Report, "Weapon Data: Fire, Impact, Explosion", Copy No. 1083.

2. Additional Engineering Data and revision sheets will be furnished by this Office, when available.

1 Incl
As in para. 1

J. M. Gruenther Lt Col
for R. C. COUPLAND
Brig. Gen., U. S. A.

Book in Opi Room

Don't let this book out of this room

CONFIDENTIAL

PAGE _____

3-1109, AF (REV 20 MAY 44)

SUBJECT: NDRC Report: "Weapon Data: Fire, Impact, Explosion (Pocket Sized Edition)"

TO: Twentieth Air Force
Room 3E 1070, The Pentagon
Attn: A-3 Combat Operations - Colonel Combs

FROM: AC/AS, M&S, Air Ordnance Office

DATE 9 APR 1945

COMMENT No. 1

LB-bm 72343

Attached hereto are the following copies of the current issue of sheets for the subject report, Copy No. 1083:

Data Sheets

1A3C
2A2* (Replaces 2A2.)
2C7

(WAA (envelope sealed)

3 Incls
As above

J. M. Grunstad, Col
for R. C. COUPLAND
Brig. Gen., U. S. A.

CONFIDENTIAL

DIVISION 2
NATIONAL DEFENSE RESEARCH COMMITTEE
Palmer Physical Laboratory
Princeton, New Jersey

WEDAPOC

8 January 1946
~~1 November 1945~~

U. S. Strategic Bombing Survey
Room 3D-1051, Pentagon Building
Washington 25, D. C.

Gentlemen:

These sheets are the final addition to the pocket-size edition of the loose-leaf notebook *Weapon Data--Fire, Impact, Explosion.*

Your copy of the notebook should be checked against the final table of contents and all sheets arranged as shown in this table of contents. All obselete sheets, replaced by revisions, should be removed from the book and destroyed.

DATA SHEETS

1A1
1A3a* (to replace 1A3a)
1A6* (to replace 1A6)
1A7a 1A7b
1B10* (to replace old 1B10*)
2A5 2C1a 2C8
3A2* (to replace 3A2)
3A2a 3A4 3A6
3A7 3A8 3A9
3E1a* (to replace both 3B1 and 3B1a)
3B1b
3B3* (to replace 3B3)
6A0
6A4* (to replace 6A4)
6A5* (to replace 6A5)
6A6* (to replace 6A6)
6B1 6B2 6C1
6C2a 6C2b 6D1
6D2 6D3 6F1
6F2 6F3 6F4

OTHER MATERIAL

Title page (to replace old title page)
Table of Contents (to replace old Table of Contents)
Foreword (to replace old Foreword)
Sources of Information for the Data Sheets

Will you please acknowledge the receipt of this material by signing and returning to this office one copy of this letter.

Very truly yours,

COPY NO.

1354,1371
1354 - Maj. Chas. C. Grote, Ordnance Dept.
1371 - Chief, Physical Damage Div.
APO 413, c/o Postmaster, N.Y.

Betty J. Meeker
Librarian
Division 2,

ams

I acknowledge receipt of the *CLASSIFIED* documents listed above, and assume full responsibility for the safe handling, storage and transmittal elsewhere of these items in accordance with existing regulations governing the handling of *CLASSIFIED* material

Date: _____ Signature: _____

DIVISION 2
NATIONAL DEFENSE RESEARCH COMMITTEE
Palmer Physical Laboratory
Princeton, New Jersey

WEDAPOC

8 January 1945
~~1 November 1945~~

U. S. Strategic Bombing Survey
Room 3D-1051, Pentagon Building
Washington 25, D. C.

Gentlemen:

These sheets are the final addition to the pocket-size edition of the loose-leaf notebook *Weapon Data--Fire, Impact, Explosion.*

Your copy of the notebook should be checked against the final table of contents and all sheets arranged as shown in this table of contents. All obselete sheets, replaced by revisions, should be removed from the book and destroyed.

DATA SHEETS

1A1
1A3a* (to replace 1A3a)
1A6* (to replace 1A6)
1A7a 1A7b
1B10* (to replace old 1B10*)
2A5 2C1a 2C8
3A2* (to replace 3A2)
3A2a 3A4 3A6
3A7 3A8 3A9
3E1a* (to replace both 3B1 and 3B1a)
3E1b
3E3* (to replace 3E3)
6A0
6A4* (to replace 6A4)
6A5* (to replace 6A5)
6A6* (to replace 6A6)
6B1 6B2 6C1
6C2a 6C2b 6D1
6D2 6D3 6F1
6F2 6F3 6F4

OTHER MATERIAL

Title page (to replace old title page)
Table of Contents (to replace old Table of Contents)
Foreword (to replace old Foreword)
Sources of Information for the Data Sheets

Will you please acknowledge the receipt of this material by signing and returning to this office one copy of this letter.

Very truly yours,

COPY NO.

1354,1371
1354 - Maj. Chas. C. Grote, Ordnance Dept.
1371 - Chief, Physical Damage Div.
APO 413, c/o Postmaster, N.Y.

Betty J. Meeker
Librarian
Division 2,

ams

I acknowledge receipt of the *CLASSIFIED* documents listed above, and assume full responsibility for the safe handling, storage and transmittal elsewhere of these items in accordance with existing regulations governing the handling of *CLASSIFIED* material

Date: _____ Signature: _____